Summer 2008

Autothermal non-catalytic reformation of jet fuel in a supercritical water medium

Jason W. Picou

Department:

AUTOTHERMAL NON-CATALYTIC REFORMATION OF JET FUEL IN A SUPERCRITICAL WATER MEDIUM

by

JASON WADE PICOU

A THESIS

Presented to the Faculty of the Graduate School of the

MISSOURI UNIVERSITY OF SCIENCE AND TECHNOLOGY

In Partial Fulfillment of the Requirements for the Degree

MASTER OF SCIENCE IN CHEMICAL ENGINEERING

2008

Approved by

Dr. Sunggyu Lee, Advisor
Dr. Kimberly H. Henthorn
Dr. John W. Sheffield

ABSTRACT

The non-catalytic reformation of jet fuel using supercritical water was studied in a specially designed 0.4-L Haynes Alloy 230 tubular reactor. Experiments were performed at a constant pressure of 24.1 MPa, a temperature of 770 ºC, and at a constant water-to-fuel ratio of fifteen-to-one by mass with various space times and oxygen flow rates. The experiments were conducted with and without air flow so as to examine the effects of the concurrent partial oxidation on the overall reformation process. The reactor effluent gas consisted of hydrogen, nitrogen, carbon dioxide, carbon monoxide, methane and ethane. Increasing space time increases the extent of the carbon gasification reaction and the resultant hydrogen and carbon dioxide gaseous concentrations; however the carbon gasification percentage reaches a limit of about 70% after a space time of 75 seconds when no oxygen was present. It was also established that the addition of sub-stoichiometric amounts of air, as an oxygen source, does not adversely affect the production of hydrogen gas under certain conditions while increasing carbon conversion and *in-situ* heat generation through partial oxidation. Carbon conversions of 86% to 94%, depending on the space time, were achieved with oxygen-to-carbon ratios of 0.4. In this thesis, the effects of space time and oxygen addition on the reformation of jet fuel are elucidated based on the experimental data.

ACKNOWLEDGEMENTS

Many people and institutions have contributed to the work outlined in the following pages. I would like to thank them for their support, experience and trust. First, I should acknowledge the financial backing that made this work possible. This project was sponsored by the U.S. Army under PE Number 0602705A through a subcontract from DRS Technical Services, Inc.

I would like to express my gratitude to my advisor, Dr. Sunggyu Lee, for all the opportunities and guidance he has given me in my academic and personal development. My thanks to all my friends in Dr. Lee's group, who provide insights, encouragement and have made my graduate school experience very enjoyable. Of course, I have to thank my family for their support, love and motivation throughout the years. The hard work and determination that went into this research are reflections of my parents, from whom I learned it.

TABLE OF CONTENTS

Page

ABSTRACT……iii

ACKNOWLEDGEMENTS……iv

LIST OF FIGURES……vii

LIST OF TABLES……viii

SECTION

1. INTRODUCTION……1

1.1. RESEARCH OBJECTIVES……1

1.2. MOTIVATION FOR RESEARCH……1

1.3. THE USE OF SUPERCRITICAL WATER PARTIAL OXIDATION……2

2. BACKGROUND……4

2.1. HYDROGEN……4

2.1.1. Hydrogen Production……4

2.1.2. Hydrogen as a Fuel……8

2.2. SUPERCRITICAL FLUIDS……10

2.3. SUPERCRITICAL WATER……13

3. APPARATUS……17

3.1. INTRODUCTION……17

3.2. THE SUPERCRITICAL WATER PARTIAL OXIDATION SYSTEM...17

3.3. SAFETY……21

3.4. ANALYTICAL EQUIPMENT……22

4. EXPERIMENTAL……..……..24

4.1. INTRODUCTION…….……24

4.2. OPERATION……...……..24

4.3. REACTANTS……26

4.4. PROCESS CHEMICAL REACTIONS……....……27

4.5. DESIGN OF EXPERIMENT……...…….30

5. RESULTS AND DISCUSSION……...…….35

5.1. EXPERIMENTAL CONDITIONS…….……...……35

5.2. EFFECT OF SPACE TIME……..…...……..35

5.3. EFFECT OF OXIDATION……...…….40

6. SUMMARY AND CONCLUSIONS……...…..……48

6.1. SUMMARY……...……48

6.2. CONCLUSIONS…….……...……48

6.3. RECOMMENDATIONS FOR FUTURE WORK…….……...…….....51

APPENDICES

A. GAS CHROMATOGRAPH RUN CONDITIONS AND CALIBRATION.…52

B. EXAMPLE OF AN HP CHEMSTATION REPORT……..……57

C. SPACE TIME CALCULATION USING THE PENG-ROBINSON EQUATION OF STATE WITH VAN DER WAALS MIXING RULES…...61

BIBLIOGRAPHY…….……...……64

VITA…….…….68

LIST OF FIGURES

Figure Page

2-1. The origin of the 42 million tons of hydrogen produced in 2003 worldwide……...……5

2-2. Phase diagram including supercritical region for water……...….11

2-3. Density change of water as a function of temperature at a pressure of 3400 psi……..…….14

2-4. Oxygen solubility in water as a function of temperature at a pressure of 3400 psi……...……14

2-5. Sodium chloride solubility in water as a function of temperature at a pressure of 3400 psi…….……..14

3-1. A schematic of supercritical water reformation and partial oxidation system at Missouri University of Science and Technology……..…….……18

3-2. A diagram of the supercritical water reactor and heater assembly……...…….19

4-1. Probability density function of the carbon number rounded to the nearest whole number as a function of the normal weight for both civilian jet fuel Jet-A and military jet fuel JP-8…….……27

5-1. Total gas composition and gasification percentage as a function of space time……...36

5-2. Nitrogen-free gas composition and gasification percentage as a function of space time……..40

5-3. Nitrogen-free product gas flow rate and gasification percentage as a function of oxygen-to-carbon molar feed ratio……..41

5-4. Nitrogen-free product gas flow rate and gaseous conversion as a function of oxygen-to-carbon molar feed ratio……..……43

5-5. Nitrogen-free product gas flow rate and gaseous conversion as a function of oxygen- to-carbon molar feed ratio……...……..……45

LIST OF TABLES

Table Page

2-1. Properties of some common fuel cells……9

2-2. Critical points of various chemical compounds……..……13

4-1. Experimental run matrix of jet fuel and air in supercritical water. ….……..…31

4-2. Heat of reaction assuming all oxygen consumed in partial oxidation and the remainder of the fuel was reformed……..….33

4-3. Hydrogen gas production per gram of fuel fed for increasing oxygen -to-carbon ratio…….……..……...…….……33

5-1. Experimental run conditions of aviation fuel and air in supercritical water…..…35

5-2. Hydrogen and carbon monoxide produced per gram of fuel for each experiment……..……46

1. INTRODUCTION

1.1. RESEARCH OBJECTIVES

The object of this research was to produce hydrogen via the non-catalytic supercritical water reformation of jet fuel. Experiments were conducted using air as an oxygen source so as to examine the effects of the concurrent partial oxidation on the overall reformation process. Oxygen deficient reaction conditions were maintained to promote the partial oxidation reaction over total combustion. The exothermic heat generated *in-situ* by partial oxidation was to provide some of the energy necessary for the endothermic reformation reaction of the jet fuel, thus approaching an autothermal mode of reactor operation. The effect of space time and oxygen level on the reformation reaction in general, and on the production of hydrogen specifically, was determined while keeping other variables such as temperature, pressure, and water to fuel ratio, constant.

1.2. MOTIVATION FOR RESEARCH

The transition from an economy dependent on fossil fuels to other forms of energy is of vital concern. Given that the supply of fossil fuel is finite, and that human consumption of energy is always increasing, it becomes evident that in the future an alternative energy form must be utilized. Also, it is becoming evident that fossil fuels may be upsetting the global climate, with the release of carbon dioxide and other greenhouse gasses that come from their combustion and use.[1] Hydrogen has been proposed as one of these alternative fuel sources. Hydrogen gas does not occur on earth in any reasonable quantity; it must be produced from compounds that contain it.[2] There

are a number of different methods to produce hydrogen, some from fossil fuels and some not. If hydrogen is used as a major fuel source, there will be need for portable, on-demand production capabilities just as there are portable electricity generators today. While in the future society may not be able to depend on fossil fuels, in the transition period there will be a need for both traditional and alternative energies. Alternative fuels produced from traditional fuel sources may be an important intermediate step in the transition to a new fuel source.

Also, portable, on-demand reformation of hydrogen from military logistics jet fuel (JP-8), coupled with a fuel cell, would enable armed forces personnel to produce electricity in the field with very little noise or heat signature. Rather than making electricity from internal combustion generators, the armed forces are considering a fuel cell because of the noise reduction. The reason for using JP-8 as the hydrogen source are logistical; the armed forces want to have one fuel that all equipment and vehicles can run on to reduce complexity when supplying field units. While the hydrogen economy may be years away, a portable hydrogen reformer would be immediately applicable for the armed forces.

1.3. THE USE OF SUPERCRITICAL WATER PARTIAL OXIDATION

There are many difficulties in the reformation of jet fuel, due to its hydrocarbon makeup and the high concentration of sulfur. Jet fuel is similar in average chain length to diesel fuel or kerosene, and contains branched and cyclic compounds. These longer chain hydrocarbons are more difficult to reform than smaller ones because of the higher energies needed to break more carbon bonds, along with the tendency of branched and

aromatic compounds to produce coke fouling at high temperatures. Sulfur is a traditional poison for catalysts, which are used in most reformation processes.

These difficulties are overcome using supercritical water partial oxidation for the reformation of jet fuel. In this process, supercritical water functions as a highly energized reforming agent and also as a homogenizing reaction medium. Supercritical water is a non-polar solvent, allowing hydrocarbons to be miscible in all proportions.[3] Oxygen is soluble in any proportion in supercritical water, while the addition of oxygen in the form of air provides *in-situ* heat generation and leads to autothermal reformation, while increasing carbon conversion and lessening coke formation.[4] The absence of a catalyst negates any possibility of sulfur poisoning.

2. BACKGROUND

2.1. HYDROGEN

It is estimated that hydrogen makes up about three quarters of the observed mass of the universe, and is the tenth most common element on earth, where it is found mostly as water. Because hydrogen gas is so buoyant it readily escapes from the atmosphere, meaning less than 1 part per million by volume of the atmosphere is free hydrogen gas.[5, 6] In 2003, world production of hydrogen gas was 42 million tons, and almost all of that was used in industrial chemical processes. Sixty percent was used to produce ammonia by the Haber-Bosch process, which is in turn used mostly to make fertilizer. Twenty three percent was used by oil refineries to upgrade and remove sulfur from fuel, and the rest was used in other chemical and metallurgical processes, as well as in the space program as a fuel. The space program is by far the largest user of hydrogen for fuel, due to its high energy to weight ratio.[7, 8]

2.1.1. Hydrogen Production. The Department of Energy's Office of Energy Efficiency and Renewable Energy explains hydrogen this way.

> "Hydrogen is an energy carrier, not an energy source. Hydrogen can store and deliver usable energy, but it doesn't typically exist by itself in nature; it must be produced from compounds that contain it."[2]

There are a number of different methods used and under development to produce hydrogen such as electrolysis and the reformation of natural gas, oil, coal, and biomass. In 2003, 42 million tons, or 500 billion standard cubic meters of hydrogen were produced.[7] The amount of hydrogen produced by these different sources is illustrated in Figure 2-1.

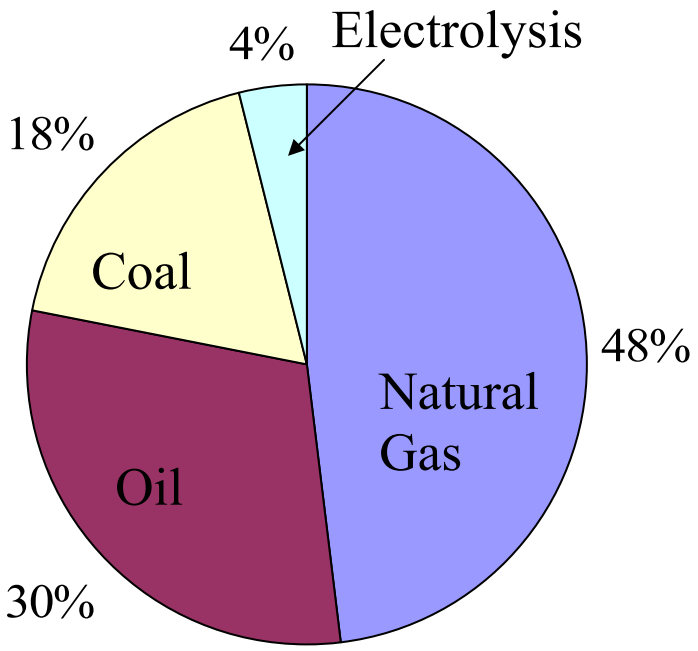

Figure 2-1. The origin of the 42 million tons of hydrogen produced in 2003 worldwide.[7]

Electrolysis uses electricity to break water into its constituents, hydrogen and oxygen. The cathode and anode, usually made from inert metal, are placed in the water and hydrogen is produced on the cathode and oxygen at the anode. Electrolysis is usually sped up by the addition of an electrolyte, such as potassium hydroxide, to the water.[9] The energy required to produce hydrogen by electrolysis (assuming 1.23 V and atmospheric pressure) is between 33 and 47 kW•h/kg H_2. There are systems that first pressurize the water to about 7000 psi, then use electrolysis to produce hydrogen. This process requires more energy (60 kW•h/kg H_2), but the hydrogen is already at an elevated pressure for storage and transport.[7] Electrolysis is simple and well tested, but since electricity must first be generated, it is not as cost effective or efficient as other methods. During the

production of hydrogen by electrolysis no greenhouses gasses are emitted, but depending on where the electricity comes from this may not always be the case.[2]

Over 95% of the hydrogen produced in the U.S. today comes from the steam reforming of natural gas. Steam reforming involves high temperature steam at a pressure of 50 to 350 psi reacting with the natural gas to form hydrogen and carbon monoxide. The carbon monoxide is further reacted with water in a reaction called the water gas shift reaction to produce more hydrogen and carbon dioxide. The reactions are given below.[10]

Reforming reaction: $CH_4 + H_2O \rightarrow CO + 3H_2$ $\Delta H°_{298} = 206$ kJ/mol (1)

Water gas shift reaction: $CO + H_2O \rightleftharpoons CO_2 + H_2$ $\Delta H°_{298} = -41.2$ kJ/mol (2)

When used in industry, both the reforming reaction and the water gas shift reaction are catalytic reactions; the reforming reaction is usually carried out at temperatures of 700 to 1100°C with a nickel catalyst on an alumina support.[11] The water gas shift reaction proceeds at much lower temperatures than the reforming reaction, 150 to 600°C, and is typically carried out over a catalyst of copper and zinc oxide on an alumina support.[12,13] The natural gas must be cleaned of sulfur and chlorine before being reformed, because these species poison the catalysts.[10] There are other processes similar to steam reforming that use some oxygen to partially combust the methane, leading to better heat transfer and higher efficiency.[14, 15] The technology behind steam reforming is well known, efficient and practiced today, but the ease of the process lies in the cleanliness of the feed stock; higher sulfur compounds and larger hydrocarbons become harder and more expensive to reform.

There are also technologies, similar to the steam reformation of methane, to reform liquid hydrocarbons like petroleum products, alcohols, and bio-oils. The technology to completely reform the smaller hydrocarbons like methanol and ethanol is more advanced than the complete reformation of larger hydrocarbons.[16, 17] As Figure 2-1 shows, 30% of the hydrogen produced worldwide comes from oil. Since the United States makes 95% of its hydrogen from natural gas, hydrogen is mostly produced this way in other countries. In oil refineries, there are catalytic reforming units that convert low-octane naphtha into higher octane products, and a byproduct of this process is hydrogen. The reaction ranges from 490°C to 530°C in temperature and 70 to 650 psi.[18, 19] This hydrogen is usually used within the refinery for fuel upgrading and hydrodesulfurization.

Another method of producing hydrogen is the gasification of coal or biomass.[2] This process has been in use for over one hundred years; before natural gas was piped across the country city lights burned gas that was made from gasified coal called town gas.[20] The process is similar to the partial oxidation of natural gas because the coal or biomass is heated under pressure and reacted with steam and oxygen to form hydrogen and carbon monoxide. There are a variety of processes to gasify coal, catalytic and non-catalytic, with temperatures varying from 620°C to 1500°C and pressures from atmospheric to 1250 psi. SASOL, a South African chemical company, is a leader in producing synthesis gas from coal.[20] Reforming coal is difficult because of the large amount of impurities like ash and sulfur, and because coal is a solid, which makes it more difficult to use in a reactor. This procedure may be able to produce hydrogen cheaply

and efficiently, but requires a large, fixed operation and substantial investments of time and money.[2]

Another option, and the topic and core of this thesis, is the generation of hydrogen from hydrocarbons using supercritical water partial oxidation. Supercritical water has benefits over the other processes such as operating on a smaller scale, higher diffusivity, organic solubility, and the ability to operate with many different fuels catalyst-free. It does not require the large infrastructure and investments that coal gasification does, and may prove to be more efficient than conventional steam reforming or partial oxidation. Supercritical water reformation would have the same on-site generation capability as electrolysis while perhaps using less energy.

2.1.2. Hydrogen as a Fuel. In order to use hydrogen, there have to be ways to generate, transport and store it, and devices or engines that turn the hydrogen into power or a desired form of energy.[21] While the generation of hydrogen was discussed in the previous section, transportation and storage are both challenges, because of the high pressures and/or low temperatures needed to store enough hydrogen gas to practically use. This is because of the low energy density of hydrogen by volume compared to hydrocarbon fuels. Also, hydrogen gas has the propensity to leak from metal containers and causes weakness to metals. Therefore, other methods including storage as metal hydrides and chemical storage along with gaseous and liquid hydrogen storage are being researched.[22]

As far as using hydrogen as a fuel, there are many different methods of converting it to usable energy. The fuel cell, which uses hydrogen and oxygen from the air to make water, heat and electricity, is one way to convert hydrogen to energy. Fuel cells are

generally more efficient than combustion engines or turbines, and have fewer moving parts and so have less likelihood of mechanical failure.[23] There are a number of different types of fuel cells, such as the Polymer Electrolyte Membrane (PEM) fuel cell, the Solid Oxide fuel cell (SOFC), the Alkaline fuel cell (AFC), and the Molten Carbonate fuel cell (MCFC), among others. Table 2-1 lists some of the common fuel cells and their capabilities.[23]

Table 2-1. Properties of some common fuel cells.[23]

Fuel cell type	Operating Temperature	System Output	Efficiency
Alkaline (AFC)	90 - 100°C	10 - 100 kW	60-70% electric
Phosphoric Acid (PAFC)	150 - 200°C	50 kW to 1 MW	80-85% overall with combined heat and power (CHP), 36-42% electric
Polymer Electrolyte Membrane (PEM)	50 - 100°C	greater than 250 kW	50-60% electric
Molten Carbonate (MCFC)	600 - 700°C	greater than 1 MW	85% overall with CHP, 60% electric
Solid Oxide (SOFC)	650 - 1000°C	5 kW to 3 MW	85% overall with CHP, 60% electric

Each fuel cell has characteristics that make it desirable in certain applications. The high temperature fuel cells like MCFC and SOFC can use small amounts of carbon monoxide as a fuel as well as hydrogen, and SOFC can also process small amounts of methane as fuel.[24] The higher operating temperature systems can use a combined heat

and power (CHP) system to increase efficiency by making use of the waste heat. The largest hurdle that fuel cells must overcome is their sensitivities to impurities in the hydrogen gas stream, and the operating temperature and weight of the fuel cells.[23]

Hydrogen can also be used directly in specially made internal combustion engines. Ever since the internal combustion engine was invented, people have tried using hydrogen as a fuel source. Hydrogen has a number of properties that makes it suitable for combustion engines, such as its ability to be burned with a low amount of oxygen, leading to lower temperatures, less pollution, greater fuel economy and more complete combustion. Also, hydrogen has a high diffusivity in air, leading to a uniform mixture of fuel and air and better combustion. There are also drawbacks to using hydrogen in a combustion engine. Hydrogen engines have to deal with pre-ignition problems due to hydrogen's lower ignition energy and wider flammability limits. There are also storage and delivery complications. There are some hydrogen internal combustion vehicles on the road today, and more are planed for the future. In general, the hydrogen internal combustion engine is seen as a bridge between the fossil fuel internal combustion engine and a hydrogen fuel cell vehicle.[8]

2.2. SUPERCRITICAL FLUIDS

A supercritical fluid is a unique state of mater that occurs for any fluid that is above its critical temperature and pressure. In general, if the temperature of a liquid is raised at constant pressure it becomes a gas, or if the pressure on a gas is increased at constant temperature it becomes a liquid. At a point called the critical point, if the temperature or pressure is raised the fluid it is no longer a gas or a liquid but is a totally

different state of mater called a supercritical fluid. It can be thought of as a fluid that has both liquid and gas-like properties. Theoretically, all compounds have a critical point, but some such as polymers degrade before reaching it.[25] The most studied supercritical fluids are carbon dioxide and water, due to their abundance, low cost, benign nature and usefulness.

The critical point was first discovered in 1822 by Baron Charles Cagniard de la Tour in an experiment that involved heated, pressurized rotating barrels that contained a small metal ball. Below the critical point the ball made a distinct noise because of the vapor-liquid interface, but above the critical point the noise changed and de la Tour hypothesized that there were no longer two separate phases but one supercritical phase.[26] Figure 2-2 below illustrates the supercritical region for water, the critical point for which is 647.3 K and 22.06 MPa.[25] While supercritical fluids have been known for a long time, there are still many applications in which they could be utilized.

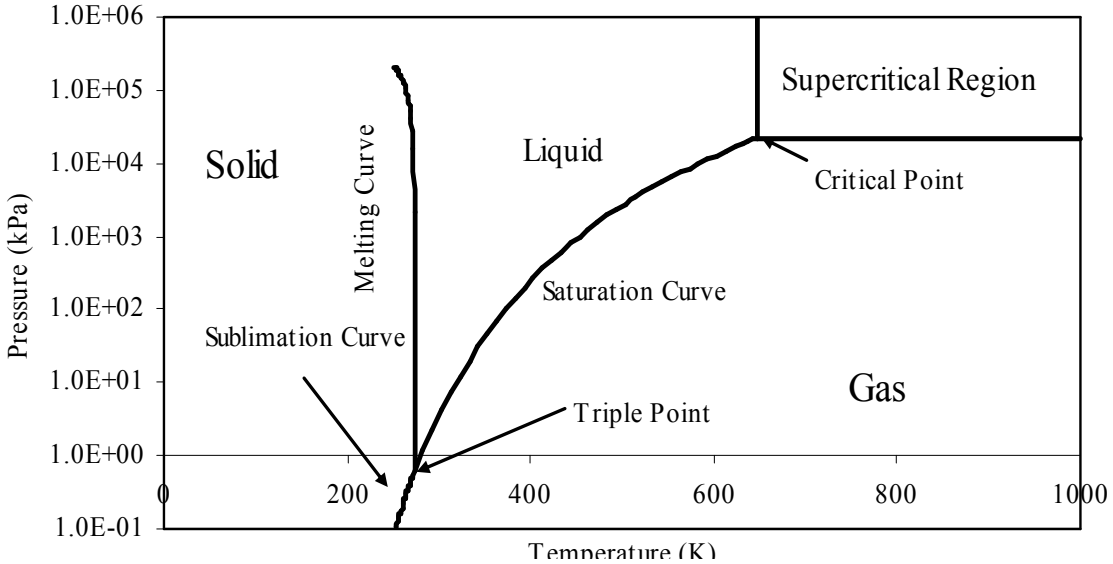

Figure 2-2. Phase diagram including supercritical region for water.

As stated above, supercritical fluids have characteristics of both liquids and gasses, which make them useful in industry and promising for future applications. A supercritical fluid, as compared to a liquid, has a higher diffusivity, a lower viscosity and no surface tension at all. The density is highly dependent on temperature and pressure near the critical point, thus allowing a wide variability in the density.[27] These properties, especially the higher diffusivity, make supercritical fluids applicable and potent solvents. Supercritical fluids are also simple to regenerate because by cooling and depressurizing the fluid it loses its supercritical solvent capabilities and the solute precipitates out, leaving the solute and solvent separated.[27] Some supercritical fluids, like water and carbon dioxide, are non-toxic and hence are widely used in the food and pharmaceutical industry. They can be readily separated out of the product, but even if some remains it is completely benign. Many other supercritical fluids such as carbon dioxide and nitrous oxide have low critical points that make it less energy intensive to employ them. Table 2-2 illustrates the critical points of some species commonly used in supercritical applications.[25] Supercritical fluids are currently used to decaffeinate coffee and tea, to extract the nicotine from tobacco, textile dying and dry cleaning, cleaning and etching silicon wafers, waste water decontamination, extraction from and impregnation of polymers, polymerization and graft copolymerization, and to make other natural food extracts, among other applications.[25, 28] The benefits of supercritical extraction become apparent considering that before supercritical carbon dioxide was used to decaffeinate coffee and tea, octanol, benzene and methylene chloride were used as solvents.[29] Carbon dioxide is both better for humans and the environment than any of these chemicals.

Supercritical fluids are also a good medium for conduction reactions such as polymerization, and some supercritical fluids actively participate in the reactions.[30]

Table 2-2. Critical points of various chemical compounds.[25]

Species	T_c (K)	P_c (MPa)
Methane	191.0	4.7
Trifluoromethane	299.1	4.9
Carbon dioxide	304.2	7.4
Ethane	305.4	4.9
Propane	369.8	4.3
Ammonia	405.6	11.3
n-Hexane	507.4	3.0
Acetone	508.1	4.7
Methanol	512.6	8.1
Ethanol	516.2	6.4
Benzene	562.2	4.9
Toluene	591.7	4.1
Water	647.3	22.1

2.3. SUPERCRITICAL WATER

Supercritical water includes the properties listed above and has some unique ones of its own. The diffusivity, density, dielectric constant, organic and inorganic solubility, and viscosity all change for supercritical water.[25] Figures 2-3, 2-4 and 2-5 illustrate how the density, gas solubility and inorganic solubility changes as a function of temperature at 3400 psi.[31]

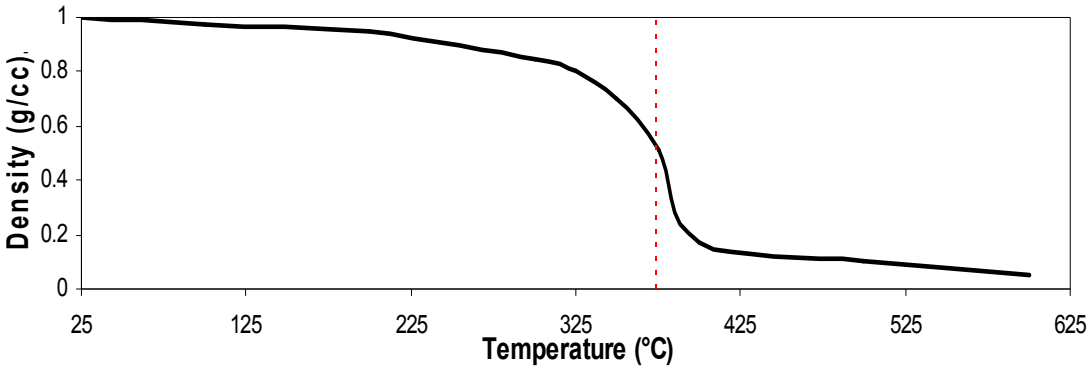

Figure 2-3. Density change of water as a function of temperature at a pressure of 3400 psi.[31]

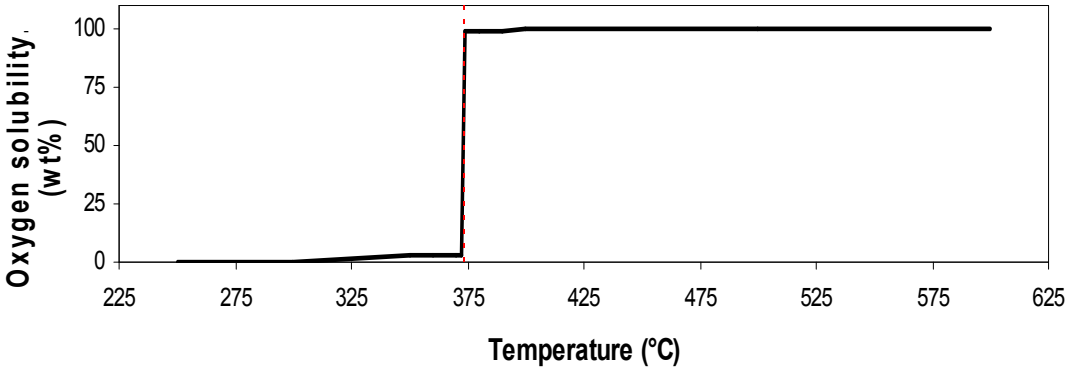

Figure 2-4. Oxygen solubility in water as a function of temperature at a pressure of 3400 psi.[31]

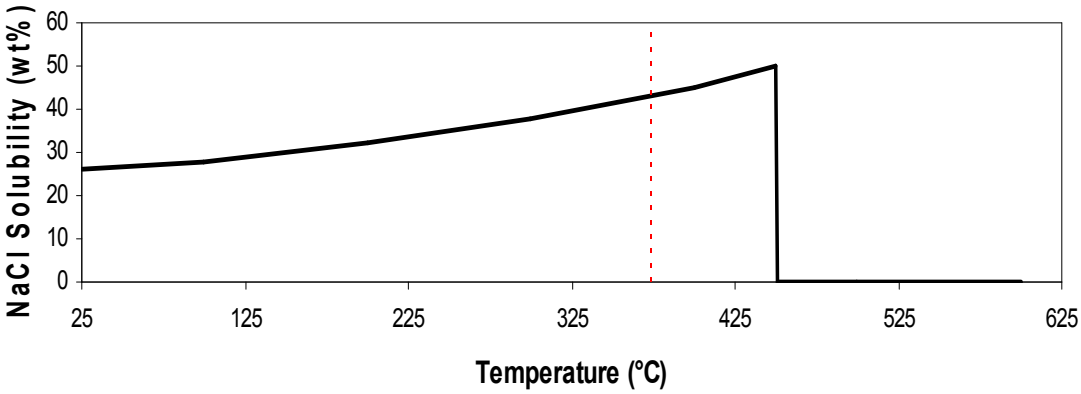

Figure 2-5. Sodium chloride solubility in water as a function of temperature at a pressure of 3400 psi.[31]

The dashed line at 375°C is the temperature at which pure water becomes supercritical. The density changes sharply around the critical point, so that small variations in temperature or pressure can have large variations in the density. As shown in Figure 2-4, gasses such as oxygen are 100% soluble in supercritical water, as are other permanent gasses such as carbon monoxide and methane.[32] Hydrocarbon solubility follows a similar pattern, water having a sparing solubility toward hydrocarbons until supercritical, at which point hydrocarbons are totally soluble.[31] Supercritical water is distinct from ambient water in that the hydrogen bonding of supercritical water is almost entirely disrupted, making it more like an organic solvent than ambient water.[33] The disrupting of the hydrogen bonding gives supercritical water a low dielectric constant, meaning supercritical water is completely miscible with non-polar compounds like hydrocarbons and chlorofluorohydrocarbons, while being immiscible to salts.

Figure 2-5 illustrates the miscibility of salts in supercritical water. The reason that the solubility increases gradually after the critical point then suddenly decreases at about 450°C is because the salt changes the critical point of water, just as it changes the boiling and melting point of water. The dashed line represents the pure water critical point, but the steep decline in solubility at about 450°C is the actual critical point for this mixture.[31] These properties of supercritical water are the complete opposite to some of the properties of ambient water, which is largely immiscible to oils, dissolves salts and can only dissolve a small amount of permanent gasses. These properties make supercritical water a promising medium for the partial oxidation of hydrocarbons, because both hydrocarbons and oxygen are soluble in supercritical water.

Supercritical water and supercritical water oxidation has been investigated for years as a medium for waste disposal, depolymerization, and the reformation of various hydrocarbons and biomass.[25, 34, 35, 36] The first industrial use of supercritical water was in a deep-shaft waste water reactor developed by Vertox in 1975, which used a deep shaft drilled into the earth to develop high pressure. A waste water stream and air were pumped down the shaft, which became supercritical due to the energy liberated *in situ* by oxidation and the high pressures due to the weight of the water above. The waste in the water was oxidized to water and carbon dioxide.[25] The first aboveground supercritical water reactor was developed by Modell and coworkers at the Massachusetts Institute of Technology in 1979 to investigate the reformation of glucose.[25, 37] Since then, numerous studies have been conducted into the applications of supercritical water.

3. APPARATUS

3.1. INTRODUCTION

The supercritical water reformation and partial oxidation system consists of a liquid feed system, integrated heat exchanger, preheat, air feed system, reactor assembly, reactor heaters, sample collection system, and data acquisition and control system. The frame is made of Unistrut and ¼" steel plate, is four feet in width, four feet in length and eight feet long and mounted on wheels for ease of transport. Most of the interior is empty space to facilitate maintenance. A schematic process flow diagram is shown in Figure 3-1. Along with the supercritical water system itself there are a few important pieces of analytical equipment that are necessary for operation and analysis.

3.2. THE SUPERCRITICAL WATER PARTIAL OXIDATION SYSTEM

The liquid feed system begins with the de-ionized water and jet fuel containers on scales so that the mass rate of change can be quantified, with Eldex high pressure micrometering pumps (models BBB and AA) used to feed the liquids and bring them to pressure. An integrated heat exchanger allows the incoming water to be heated by the reactor effluent, thus increasing efficiency. After the integrated heat exchanger, the fuel is mixed with the water and preheated with Omega heat tapes before entering the reactor at the inlet cross, where the air feed also enters the reactor. The air feed system consists of an Airgas Breathing Quality Grade D compressed air tank connected to a pneumatic high pressure Haskel gas booster, which increases the air pressure to 5000 psi in a subsequent air storage bomb. The storage bomb acts as a reserve and also to dampen any

pressure pulses from the gas booster. A pneumatically operated Badger control valve and a Brooks mass flow meter, with the Labview software on the systems computer, provide air flow control into the reactor assembly.

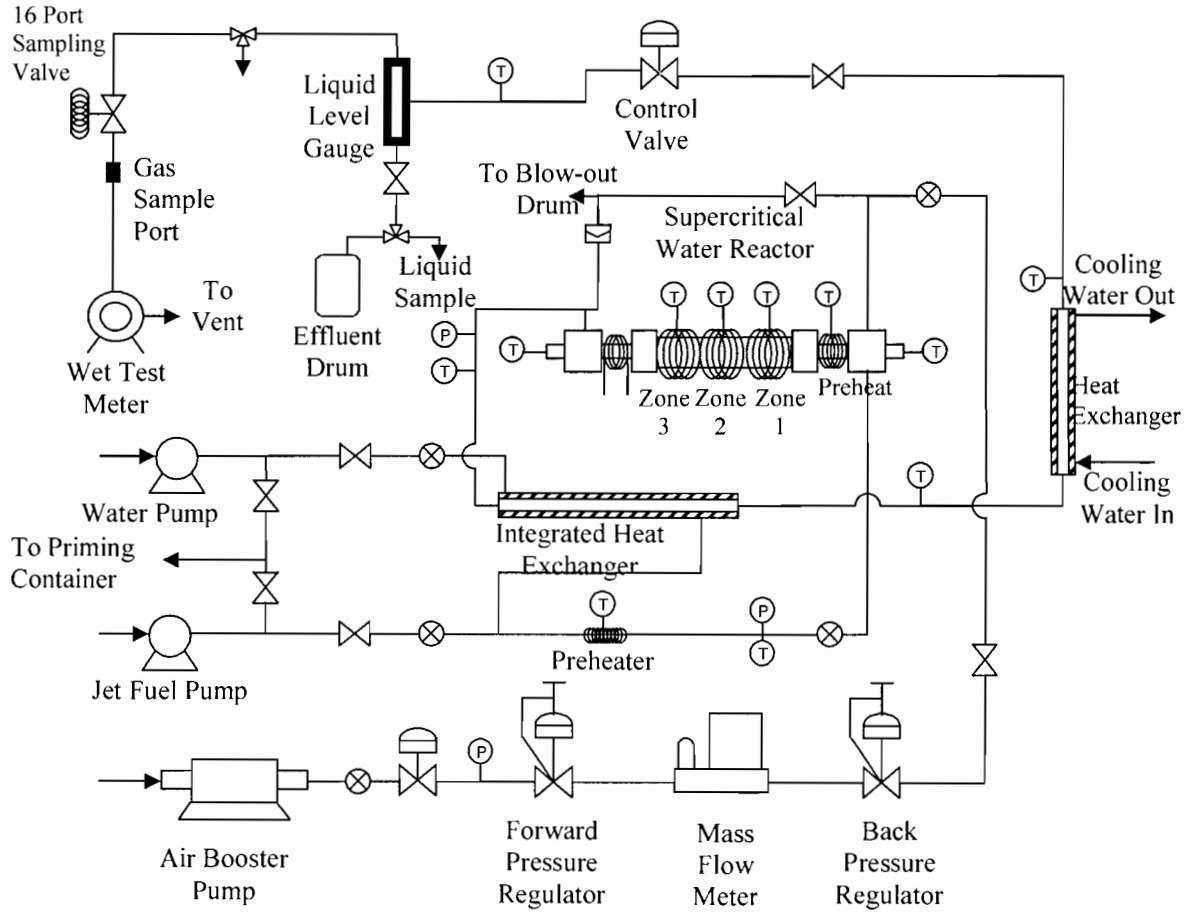

Figure 3-1. A schematic of supercritical water reformation and partial oxidation system at Missouri University of Science and Technology.

The reactor assembly consists of an inlet cross, an inlet reactor head, the reactor body, an outlet reactor head and an outlet cross. Two screw caps screw into the reactor and hold each of the reactor heads to the reactor. There are also two thermowells, one each for the inlet and outlet, which extend through the crosses and down the length of the

reactor and provide internal temperature measurements of the reactor. Figure 3-2 illustrates the reactor and heater assembly, as well as the locations of the reactor thermocouples (RTC), which are placed inside the thermowell to record the internal temperature of the reactor.

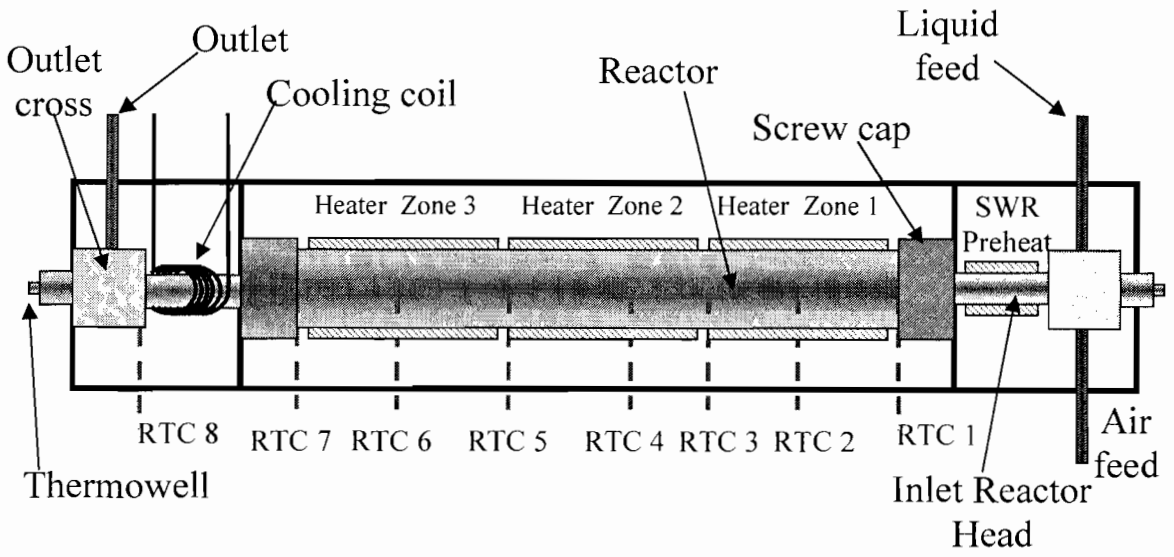

Figure 3-2. A diagram of the supercritical water reactor and heater assembly.

The reactor body, the inlet and outlet reactor heads, the screw caps, and the thermowells were manufactured by Parr Instrument Co. and the inlet and outlet crosses and thermowell adapters were manufactured by the High Pressure Equipment Co. The reactor body has a 3" O.D and a 1" I.D., and is 36" long. When fully assembled, the entire reactor assembly is 61.3" long, and has an internal volume of about 380 mL. The crosses are connected to the head assemblies and tubing with coned and threaded fittings, and the head assemblies are connected to the reactor with Graphoil gaskets and the screw caps.

The material of construction is Inconel 625 Grade 1 for the inlet and outlet crosses and Inconel 625 Grade 2 for the screw caps. The reactor body and reactor heads are made of Haynes Alloy 230. Inconel 625 Grade 1 and 2 is an alloy of 58% Nickel, 20-23% Chromium, a maximum of 5% Iron, 8-10% Molybdenum, 3.2-4.2% Niobium, with other species representing less that 1%. The difference between Grade 1 and 2 is that Grade 2 has been heat treated to improve strength and allow for higher operating temperatures and pressures.[38] Haynes alloy 230 is made of 57% Nickel, 22% Chromium, 14% Tungsten, 2% Molybdenum, a maximum of 5% Cobalt, a maximum of 3% Iron, with other species representing less than 1%.[39] These materials allow for the reactor body and reactor heads to operate over a wide range of temperatures and pressures, up to 800°C and 5250 psi. The Inconel crosses can operate up to 650°C at 5000 psi.

The heaters and insulation for the reactor were manufactured by Watlow Electric Manufacturing and come in three pieces, the inlet SWR preheat, the main reactor heater and the outlet insulation. The inlet reactor head is heated by the SWR preheat, and the reactor body by a heater which has three different heating elements, or Zones, along the reactor length to provide a uniform temperature profile in the reactor body. The outlet reactor head and cross are only insulated, and there is a cooling coil on the outlet reactor head that provides cooling in case the temperature is above the limits of the outlet cross.

The reactor effluent passes through the integrated heat exchanger where it is cooled, and is further cooled to ambient temperature in a water-fed heat exchanger. The effluent is filtered using Swagelok 90 and 15 micron filters, and then depressurized using a pneumatically operated, computer controlled, Badger control valve. The depressurized effluent is separated into liquid and gas in a Strahman Sight Gauge. The liquid is either

drained into an effluent drum or sampled, while the gas proceeds to a gas sampling port and sampling valve. From here gas samples can be analyzed in real time, or stored in a 16-port Valco sampling valve for later analysis. A Precision Scientific wet test meter measures the gas flow rate, after which it is safely vented outside the building.

National Instruments Labview software acts as the data acquisition and control system, which collects the date, time, temperature, pressure, and inlet air flow data among others and controls the heaters, reactor pressure and air flow rate. The temperature inside the reactor is controlled by monitoring the reactor thermocouples in the thermowells inside the reactor and proportionally controlling the reactor heaters to maintain the desired internal temperatures. Thermocouples are also placed on the outside of the reactor to ensure the heater's temperature range is within the safety limits of the reactor. The pressure of the reactor is controlled by the Badger control valve via PID control in response to changes in the pressure and the air flow rate is controlled via PID control by a Badger control valve in response to the measured flow rate given by the Brooks flow meter.

3.3. SAFETY

Because of the extreme conditions under which the reformer can operate, and the nature of its products, a number of safety features have been incorporated into the design of the supercritical water reformer. First, the system is contained within a ventilated 4'x4'x8' box made of ¼" steel plate. The system is prevented from going past its set and design temperature and pressure by algorithms in the Labview control software, which is backed up by independent and redundant solid state relays. A rupture disk at the exit of

the reactor provides even more insurance against overpressure and temperature. The rupture disk, if it were to fail, is connected to a vented expansion drum so that any gasses would be safely vented and all liquids collected and contained. There are also manual depressurization valves on both the inlet and the outlet that the operators can employ. In case of a combustible gas leak inside the reactor, there are combustion monitors linked to the control system that both warns the operator and shuts down the system. There are also carbon monoxide monitors strategically placed outside the system.

3.4. ANALYTICAL EQUIPMENT

Analysis of the gaseous effluent was performed using a HP 5890 Series A gas chromatograph (GC) with a thermal conductivity detector (TCD). The carrier gas for the gas chromatograph was Airgas Ultra-pure Carrier Grade Argon with a purity of 99.9995%. The TCD utilizes a 15' by 1/8" stainless steel 60/80 Carboxen 1000 packed column, which is calibrated to detect hydrogen, nitrogen, carbon monoxide, methane, carbon dioxide, acetylene, ethylene and ethane. The GC is connected to a computer that uses HP Chemstation software to control the GC. This software allows different run conditions to be saved and reused, and are called methods. There are three methods used with the GC, viz., Air02, Air03 and Loop05, which are adopted depending on the species to be detected and whether a sample loop or syringe sample is being analyzed. The GC was calibrated with gas standards and pure gasses, from which the composition of the effluent gas was determined. Appendix A lists the GC conditions and detectable species for each method, along with the residence time and calibration plot for each species. After every syringe injection or sample loop analysis, a report is generated by HP

Chemstation that gives the residence time and area of each peak, from which the species and number of moles can be determined. An example of the report generated by HP Chemstation is given in Appendix B.

4. EXPERIMENTAL

4.1. INTRODUCTION

This chapter provides details as to the real time operation of the supercritical water reformer, the materials used, the chemical reactions that may occur during supercritical water reformation and the experimental matrix. The start up, operation and shut-down of the reactor is elaborated to provide the reader an in-depth perspective on how and wherefrom the data was collected. The materials used are important as a starting point for understanding the final products. The major chemical reactions are outlined so that the products in the effluent gas can be linked to these specific reactions and explain some of the routes and origins leading to non-gaseous products. The reasoning behind the choice of experiments, with the goal of understanding the effects of space time and air flow on the reactions, will be explained and justified.

4.2. OPERATION

The operation of the supercritical water reformer begins with starting Labview, the computer data acquisition and control program. The reactor heaters are energized and their temperature set points are entered. While the reactor is warming up, the water and fuel pumps are connected and primed. The water pump and preheater heat tapes are turned on at the same time, and the pressure set point is entered through Labview. Fuel is fed once the system reaches the desired temperature and pressure. If the experiment requires air flow, then the Haskel booster pump is activated and the desired air flow rate is set into Labview and air flow begins concurrently with fuel flow. The liquid effluent is

observed through the Strahman Sight Gauge and manually drained into a collection container periodically, to prevent the sight gauge from overfilling. Samples of the liquid effluent can be taken by diverting the liquid from the collection container to a sample container using a three-way valve. Liquid samples are taken at least twice during each experiment. During the experiment, the water and fuel flow rates are monitored periodically by recording the change in mass of the respective liquid containers.

The gaseous effluent is routed through a wet test meter and the flow rate is periodically measured and recorded. Gas samples are taken with a syringe and injected into the GC for analysis. Also, gas samples are taken with a 16-port Valco gas sample loop, which allows the samples to be stored and analyzed later by the GC. An experiment is concluded when three consecutive syringe gas samples give similar molar compositions and the gas effluent flow rate is constant. Only the data collected while the gaseous effluent composition and flow rate are constant is included for that experiment, and any data previous to this is not. This is to make sure that the experiments were conducted at steady state. After the composition and flow rate become constant and the experiment is concluded, another experiment could be conducted by varying the temperature, pressure, flow rate, or all three together. In this manner, many experiments can be performed in a day.

When the experiments are concluded and the system to be turned off, first the fuel and air flow is stopped and the heaters turned off. The water flow continues so as to remove any fuel and combustible gasses from the reactor. After about fifteen minutes of

water cleaning, the water pump is turned off and the system is depressurized by opening the emergency depressurization valves and draining the contents of the reactor to the ventilated expansion drum.

4.3. REACTANTS

Three reactants are used in the supercritical water reformer for these experiments: water, jet fuel and air. The water used was deionized water from a Culligan exchange tank de-ionizer. The air feed system uses Airgas Breathing Quality Grade D compressed air from a pressurized tank. Two different jet fuel types were used in the experiments, civilian jet fuel, Jet-A, and military jet fuel, JP-8, both of which are an assortment of hydrocarbons including straight chain, branched and cyclic. An ASTM D2887 boiling range distribution analysis determined that the length of the carbon bonds varied from five to twenty carbons, with the average carbon number being twelve for both fuels.[40] Therefore, the aviation fuel was modeled as a single representative molecular species, n-dodecane, which has the chemical formula $C_{12}H_{26}$. Figure 4-1 below illustrates the distribution of carbon atoms in each fuel's hydrocarbons. Both jet fuels were sent to Texas Oil Tech Laboratories, which tested them for sulfur content and found that the civilian jet fuel (Jet-A) contained 0.099 weight percent sulfur, or 990 parts per million. The military jet fuel (JP-8) contained 0.081 weight percent sulfur, or 810 parts per million. Because these fuels are similar in bond length, boiling point distribution and sulfur content, they are considered identical for these experiments and the process study. The reason two different types of jet fuel were used was due to problems acquiring additional military jet fuel.

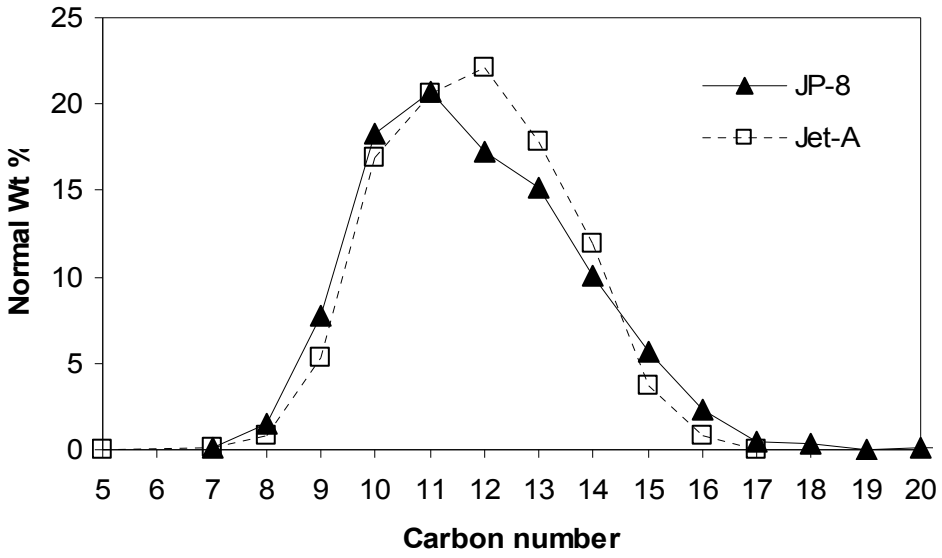

Figure 4-1. Probability density function of the carbon number rounded to the nearest whole number as a function of the normal weight for both civilian jet fuel, Jet-A, and military jet fuel, JP-8.

4.4. PROCESS CHEMICAL REACTIONS

A variety of reactions are possible in supercritical water reformation, the most important of which are illustrated below. The overall reformation reaction of jet fuel may be written as:

$$C_{12}H_{26} + 12\ H_2O \rightarrow 12\ CO + 25\ H_2 \qquad \Delta H°_{298} = 1866\ \text{kJ/mol} \qquad (3)$$

where jet fuel is represented by n-dodecane for stoichiometric simplicity based on its most prevalent molecular formula, as explained previously. The endothermic reformation reaction is the desired reaction because, due to the participation of water, about twice as much hydrogen is liberated through reformation than was contained in the

original hydrocarbon. Reformation also produces carbon monoxide, the importance of which will be discussed later. The above reaction is in competition and occurs in parallel with the pyrolysis reaction:

$$C_{12}H_{26} \rightarrow C_aH_b + C_xH_y + p\ H_2 \qquad (12 = a + x \text{ and } 26 = b + y + 2p) \qquad (4)$$

The pyrolysis reaction is endothermic, but much less so than the reformation reaction, requiring about 70 kJ/mol depending on the size of the fragments. The pyrolysis reaction is thought to be primarily responsible for any gaseous hydrocarbons contained in the effluent gas, such as methane or ethane. Repeated pyrolysis leaves hydrogen deficient fractions, which eventually become solid coke or function as coke precursors.[41]

In the presence of oxygen, another set of reactions occur. The first reaction, Equation (5), is the partial oxidation of hydrocarbons, while the second, Equation (6), is the complete oxidation reaction:

$$C_{12}H_{26} + 6\ O_2 \rightarrow 12\ CO + 13\ H_2 \qquad \Delta H°_{298} = -1036 \text{ kJ/mol} \qquad (5)$$

$$C_{12}H_{26} + 18½\ O_2 \rightarrow 12\ CO_2 + 13\ H_2O \qquad \Delta H°_{298} = -7575 \text{ kJ/mol} \qquad (6)$$

Partial oxidation is the preferred reaction because both hydrogen and carbon monoxide are the products, while total oxidation produces water and carbon dioxide, which are unwanted and wasteful. The partial oxidation reaction produces less hydrogen per mole of fuel in comparison to the reformation reaction, but is an exothermic reaction.

Both exothermic reactions would provide *in-situ* thermal energy for the reformation reaction, thereby decreasing the amount of external energy to be supplied.

In addition to these reactions, the water gas shift reaction can also occur. The water gas shift (WGS) reaction is a reversible reaction between carbon monoxide and water to produce carbon dioxide and hydrogen. The forward reaction, as described below, is exothermic, while the reverse reaction would be endothermic. This would be a highly desirable reaction, if properly managed, since additional hydrogen is produced. The forward reaction is thermodynamically favored at temperatures of 815°C or below:[20]

$$CO + H_2O \rightleftharpoons CO_2 + H_2 \qquad \Delta H°_{298} = -41 \text{ kJ/mol} \qquad (2)$$

The water gas shift reaction is an important industrial reaction of practical significance, and is usually catalyzed by either an Fe_2O_3-Cr_2O_3 or a Cu-ZnO catalyst, depending on the temperature.[42] If the water gas shift reaction proceeds as a companion reaction during supercritical water reformation, it would be doing so without any catalyst.

All these reactions do not occur alone or independently as isolated events, nor are they mutually exclusive. It could be that pyrolysis or oxidation breaks down the original jet fuel hydrocarbons, then reformation occurs on the resulting pieces. Various other reactions, like methanation or the Boudouard reaction, could also be possible, even though the thermodynamic equilibrium for the forward reaction of the former is not favorable for the process conditions of the current study. The discussion was limited to the aforementioned reactions for simplicity and because they effectively and accurately describe all of the products observed.

4.5. DESIGN OF EXPERIMENT

The space time of the fluid in the reactor and the flow rate of air into the reactor were varied to investigate how they affect the effluent gas composition and fuel conversion. The space time was varied by changing the inlet water and fuel flow rate and calculated as a function of inlet fluid density using the Peng-Robinson equation of state with the van der Waals mixing rule. The Peng-Robinson equation of state, along with the van der Waals mixing rule and a walk through of the space time calculation, is given in Appendix C. The temperature was held at 770°C, while a constant pressure of 24.1 MPa and a fifteen-to-one water-to-fuel mass ratio was maintained.

While the water and fuel flow rates are varied between experiments in order to provide different residence times, the ratio of water-to-fuel by mass was always kept at fifteen-to-one. This corresponds to about a twelve-to-one water-to-carbon (H_2O/C) molar ratio, or an aqueous aviation fuel concentration of 6.25 wt%. Stoichiometrically, there was twelve times the amount of water needed than the theoretical amount required in Equation (3). Air flow into the reactor was set so that the same oxygen-to-carbon (O_2/C) ratio would be maintained despite the changing fuel flow rates. The oxygen-to-carbon ratio is a measure of how much oxygen was fed per minute divided by how much carbon was fed per minute. Table 4-1 outlines the water, fuel, and air flow rates, with the corresponding oxygen-to-carbon ratio and space time, for a given experimental run. The experiments were conducted in the randomized order given by the experiment ID, from one to twelve.

Table 4-1. Experimental run matrix of jet fuel and air in supercritical water. Temperature was constant at 770°C and pressure at 24.1 MPa. The space time and the molar oxygen-to-carbon ratio are varied.

Experiment ID	Water Flow (g/min)	Jet Fuel Flow (g/min)	Air Flow (slpm)	Molar Oxygen-to-Carbon Ratio (O_2/C)	Space Time (sec)
3	7.5	0.5	0.0	0.00	160
4	7.5	0.5	0.2	0.07	156
7	7.5	0.5	0.5	0.13	151
6	7.5	0.5	1.5	0.40	135
11	15.0	1.0	0.0	0.00	80
10	15.0	1.0	0.5	0.07	78
9	15.0	1.0	1.0	0.13	75
8	15.0	1.0	3.0	0.40	67
1	30.0	2.0	0.0	0.00	40
12	30.0	2.0	1.0	0.07	39
2	30.0	2.0	2.0	0.13	38
5	30.0	2.0	6.0	0.40	34

Experiments 3, 11 and 1 are carried out without air flow and allow analysis of the effects of space time on the reformation reaction without oxygen. In general, the experiments conducted at similar space times with increasing air flow will be grouped together by the average space time for each group. For example, experiments 3, 4, 7 and 6 will be identified as the 150 second space time experiments; experiments 11, 10, 9 and 8 will be the 75 second space time group, 1, 12, 2 and 5 will be the 37 second group. The reason the space time decreases within a group was because the water and fuel flow rate was kept constant while increasing the air flow, which decreases the space time. Each group illustrates the effect of increasing the oxygen-to-carbon ratio. Each group was increased by the same ratio to make comparison between the groups easier.

The oxygen-to-carbon ratio affects Equation (5), the partial oxidation reaction. With the jet fuel modeled as $C_{12}H_{26}$, the minimum ratio necessary to partially oxidize all the fuel, assuming the reaction continues to completion without any other competing reactions, is an oxygen-to-carbon ratio of 0.5. An O_2/C ratio of 0.4 would partially oxidize 80% of all incoming fuel given these same assumptions. All the experiments were conducted below this theoretical minimum of 0.5 O_2/C in order to limit the partial and total oxidation reactions. As the oxygen-to-carbon ratio increases, the amount of energy liberated by the oxidation reactions increases and the proportion of fuel left to participate in the endothermic reformation reaction decreases. This leads to the autothermal nature of the reactions, in that more energy is liberated through the oxidation reactions than is used in the reformation reaction. The amount of oxygen that is needed so that the energy requirements of the reformation reaction equals the energy liberated by the partial oxidation reaction, again assuming that all oxygen is consumed in partial oxidation and all fuel not so consumed is reformed, is equal to a 0.32 oxygen-to-carbon ratio. Because the reformation reaction is more endothermic than pyrolysis, when it is assumed that all fuel not oxidized is being reformed it creates an upper bound for the amount of heat needed. Because partial oxidation is less exothermic than total oxidation, assuming that the oxygen is consumed in partial oxidation makes a lower bound for the amount of heat generated. Table 4-2 shows the heat of reaction given the above assumptions. Experiments 5, 6 and 8 all have oxygen-to-carbon ratios higher than 0.32, meaning more energy is produced by oxidation than used by reformation in these reactions. Energy is still necessary to bring the reactants up to the reaction temperature, so external heat sources are still needed.

Table 4-2. Heat of reaction assuming all oxygen consumed in partial oxidation and the remainder of the fuel is reformed.

Experimental ID	Molar O_2/Carbon ratio	Heat of reaction (kJ/min)
3	0.00	5.5
4	0.07	4.3
7	0.13	3.2
6	0.40	-1.3
11	0.00	11.0
10	0.07	8.7
9	0.13	6.4
8	0.40	-2.7
1	0.00	21.9
12	0.07	17.4
2	0.13	12.8
5	0.40	-5.3

While partial oxidation produces heat, it also produces less hydrogen, the production of which is one of the goals of these experiments. Table 4-3 below illustrates how much hydrogen production would be affected by the increasing oxygen flow rate. Units of grams of hydrogen produced per gram of fuel fed will be used so that the separate space times can all be compared at once, since they have the same theoretical production on that basis and the same oxygen-to-carbon ratios.

Table 4-3. Hydrogen gas production per gram of fuel fed for increasing oxygen-to-carbon ratio.

Molar O_2/Carbon ratio	Grams of H_2 produced per gram of fuel fed
0.00	0.30
0.07	0.28
0.13	0.26
0.40	0.18

As illustrated in the above table, the addition of oxygen does reduce the amount of hydrogen produced, there being about 38% less hydrogen when the oxygen-to-carbon ratio is at 0.40 than when no oxygen is present. This decrease in hydrogen production is the price paid for the *in-situ* heat generated by the addition of air. These numbers represent theoretical maximums, if all the previous assumptions are met, and will be used to compare with the actual experiments.

5. RESULTS AND DISCUSSION

5.1. EXPERIMENTAL CONDITIONS

The twelve experiments proposed in the experimental section were conducted and Table 5-1 illustrates the actual temperatures, pressures, flow rates, space times and fuel types for each experiment. While great care was taken to ensure experiments were performed according to the run matrix outlined in the Experimental section, there was a slight variation between the proposed experiments and the actual experimental conditions due to both human error and the tolerances of the control parameters.

Table 5-1. Experimental run conditions of aviation fuel and air in supercritical water.

Run ID	Fuel type	Water flow (g/min)	Fuel flow (g/min)	Air flow (slpm)	Temperature (°C)	Pressure (MPa)	Space time (sec)
3	Jet-A	7.6	0.53	0.00	765	24.1	159
4	Jet-A	7.6	0.53	0.25	765	24.0	153
7	JP-8	7.3	0.48	0.50	763	24.1	156
6	JP-8	7.5	0.48	1.50	763	24.0	136
11	JP-8	15.1	0.93	0.00	770	24.0	79
10	JP-8	15.1	0.95	0.50	772	24.0	77
9	JP-8	15.1	0.95	1.00	772	24.1	74
8	JP-8	14.3	1.00	3.01	765	24.1	70
1	Jet-A	31.1	1.97	0.00	768	24.2	39
12	JP-8	29.6	1.94	1.00	773	24.1	39
2	Jet-A	31.5	2.00	1.99	772	24.2	36
5	JP-8	29.7	1.91	5.99	765	24.2	34

5.2. EFFECT OF SPACE TIME

Three experiments, 1, 11, and 3, at three different space times of 39, 79 and 159 seconds respectively, were conducted without air flow at an average temperature of

768±2°C and pressure of 24.1±0.1 MPa. The net effect of the variation in space time on the gas composition and gasification percentage is illustrated in Figure 5-1. The gasification percentage is a measure of how much of the liquid fuel was converted to the gas phase.

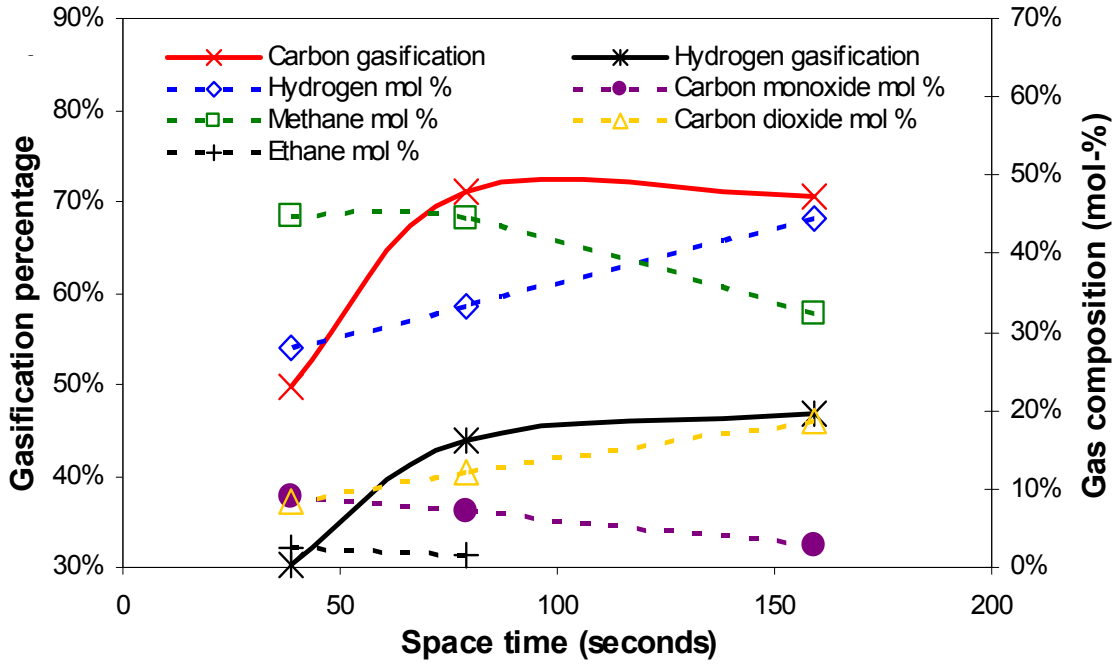

Figure 5-1. Total gas composition and gasification percentage as a function of space time. Experimental conditions, T = 770±2°C, P = 24.1±0.1 MPa, aqueous aviation fuel concentration = 6.1±0.4 wt %.

Since jet fuel is made up of carbon and hydrogen, a gasification percentage for each species can be defined. For carbon, it is the ratio of carbon in the gas phase divided by the amount that would have been present if all of the fuel was reformed according to Equation (3). The carbon in the gas phase includes that present in methane, ethane, carbon monoxide and carbon dioxide. This is a measure of carbon gasification by any

reaction, pyrolysis, reformation, oxidation or any other, compared to the theoretical maximum. The hydrogen gasification percentage for this figure, is again the ratio of hydrogen in the gas phase, which includes methane, ethane, and hydrogen gas, divided by the amount that would have been present if all of the fuel was reformed according to Equation (3) and if all the carbon monoxide produced by Equation (3) went through Equation (2), the water gas shift reaction, and produced hydrogen.

When experiments are conducted with oxygen, the hydrogen gasification percentage will be based on all of the oxygen fed being consumed in partial oxidation, the remainder of the fuel being reformed and all carbon monoxide produced by these reactions undergoing water gas shift and producing hydrogen. The reason to include the partial oxidation reaction in the definition is that partial oxidation produces less hydrogen than reformation. This definition of hydrogen gasification is the maximum amount of hydrogen that could be produced from the five principal reactions thought to occur, assuming all oxygen fed is consumed in partial oxidation. Because the GC used could not differentiate between oxygen and nitrogen, the assumption that all oxygen fed was completely consumed will be made throughout.

The carbon gasification percentage began at 50% for the shortest space time of 39 seconds and increased to 71% for the intermediate space time of 79 seconds, which was a 43% increase. It then decreased slightly to 70% for the longest space time of 159 seconds. Even though the space time of the fluid in the reactor was doubled from 79 to 159 seconds, the carbon gasification percentage did not change. This indicates that the gasification of aviation fuel had reached some sort of limit around the space time of 79 seconds, with longer space times still unable to convert more than 70% of the fuel into

gas. The 30% carbon remaining would then be in either the liquid phase or have become solid due to the pyrolysis reaction. Total organic carbon analysis of previous, similar experiments determined that less than 1% of the carbon that was fed into the system left via the liquid effluent, so if the carbon does not leave the reactor as gas it stays behind as solid. On occasion this solid has been removed from the reactor, but since the reactor was not cleaned after every run it is impossible to know exactly how much solid each experiment created. The solid recovered from these experiments has not been analyzed, but sixteen previous solid samples from run conditions similar to the current conditions have been. The average carbon weight percentage over these sixteen samples was 98.7±0.3%, with a corresponding 1.3±0.3% hydrogen percentage. It is assumed that the solid removed after performing the more recent experiments is analogous to that of the previous experiments. Therefore, when there is carbon gasification of 70%, about 30% of the carbon is pyrolysized into solid and remains in the reactor.

The hydrogen gasification percentage began at 30% and increased to 44% for the 79 second space time experiment, a 45% increase. It increased again to 47% for the 159 second space time, which was only a 7% increase. The hydrogen gasification increases slightly as the space time changes from 79 to 159 seconds, while carbon gasification does not. This could be due to an increased water gas shift reaction and increased reformation of gaseous hydrocarbons such as methane and ethane. The water gas shift reaction could be responsible for the decrease in carbon monoxide and increase in carbon dioxide and hydrogen gas concentrations, illustrated in Figure 5-1. The water gas shift reaction would not affect carbon gasification because both products and reactant are gaseous carbon.

The amount of methane and ethane decreases with increasing space time, which is indicative of enhanced reformation of the gaseous hydrocarbons at the longer space time. No ethane was detected at the longest space time of 159 seconds. The reformation of these two species produces more hydrogen in the product gas, but does not change the carbon gasification percentage since both the reactants and products have the same amount of carbon in the gas phase. The decrease in the gaseous hydrocarbons without a corresponding increase in the carbon gasification means that the gaseous hydrocarbons are being reformed preferentially over the solid carbon that was in the system. This finding emphasizes the importance of further reformation of the light hydrocarbon species, before they eventually function as coking precursors.

The effect of space time at a particular oxygen-to-carbon ratio can also be analyzed. Only the 0.4 O_2/C ratio will be analyzed because similar trends exist when comparing the effect of space time on the other oxygen-to-carbon ratios. Figure 5-2 illustrates how space time affects the gasification percentages and the gas composition when the oxygen-to-carbon ratio was kept constant. The three data points correspond to experiments 5, 8 and 6 from left to right. The carbon and hydrogen gasification percentage increases with increasing space time, as does the effluent gas hydrogen and carbon dioxide composition. The methane, ethane and carbon monoxide composition decreases. When comparing Figure 5-2 to the effect of space time without oxygen, as shown in Figure 5-1, the carbon and hydrogen conversion continues to increase and no noticeable plateau or limit was reached. There are also similarities, such as how the gas composition changes, with more hydrogen and carbon dioxide and less methane and carbon monoxide at the longer space time.

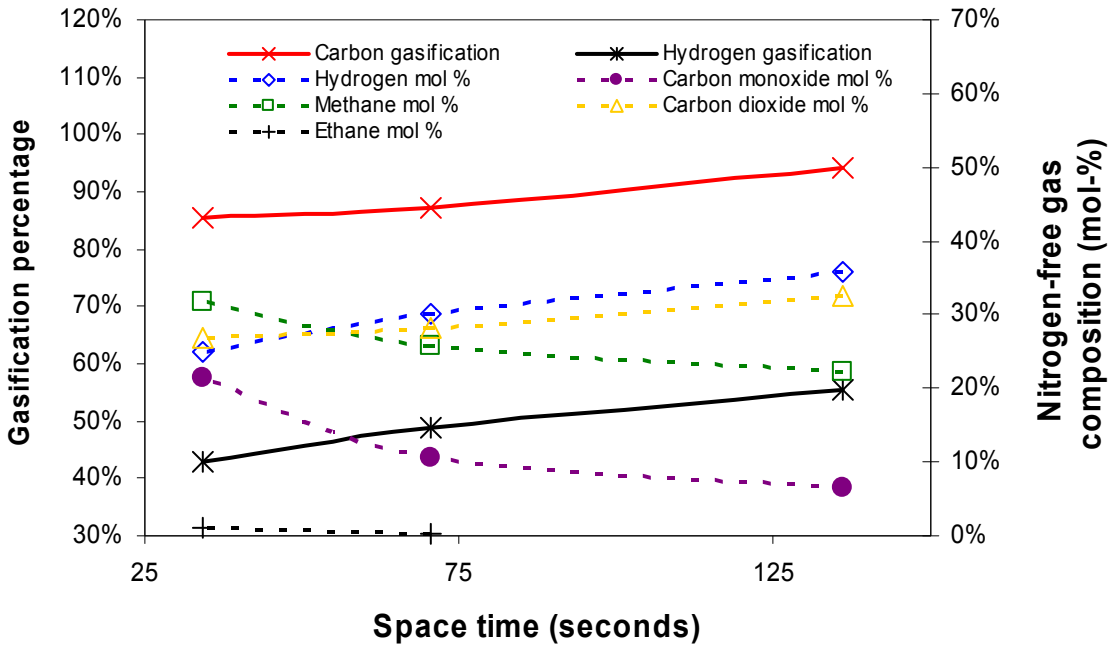

Figure 5-2. Nitrogen-free gas composition and gasification percentage as a function of space time. Experimental conditions, T = 764±1°C, P = 24.1± 0.1 MPa, oxygen to carbon ratio = 0.411±0.009, aqueous aviation fuel concentration = 6.2±0.3 wt %.

That carbon gasification continues to increase, while when no oxygen was present it remained relatively unchanged between 79 and 159 seconds at about 70%, could be due to the oxidation reaction gasifying more of the solid coke or fuel. The hydrogen gas composition increases with increasing space time, indicating that the oxidation reactions do not consume more hydrogen given a longer residence time in the reactor, and that reformation or the water gas shift reaction may be improved with increased space time.

5.3. EFFECT OF OXIDATION

Figure 5-3 depicts the gasification percentage and nitrogen-free product gas flow rate of each species as a function of oxygen-to-fuel ratio for the runs conducted at a space time of 151±10 seconds, as represented by experiments 3, 4, 7, and 6. The carbon

gasification percentage increases linearly from 70% to 94%; a 34% increase from no oxygen present to a 0.4 oxygen-to-carbon ratio. The addition of oxygen increased carbon gasification, either through oxidizing the solids formed through pyrolysis or oxidizing the fuel directly and leaving less fuel to be pyrolyzed, or a combination of the two.

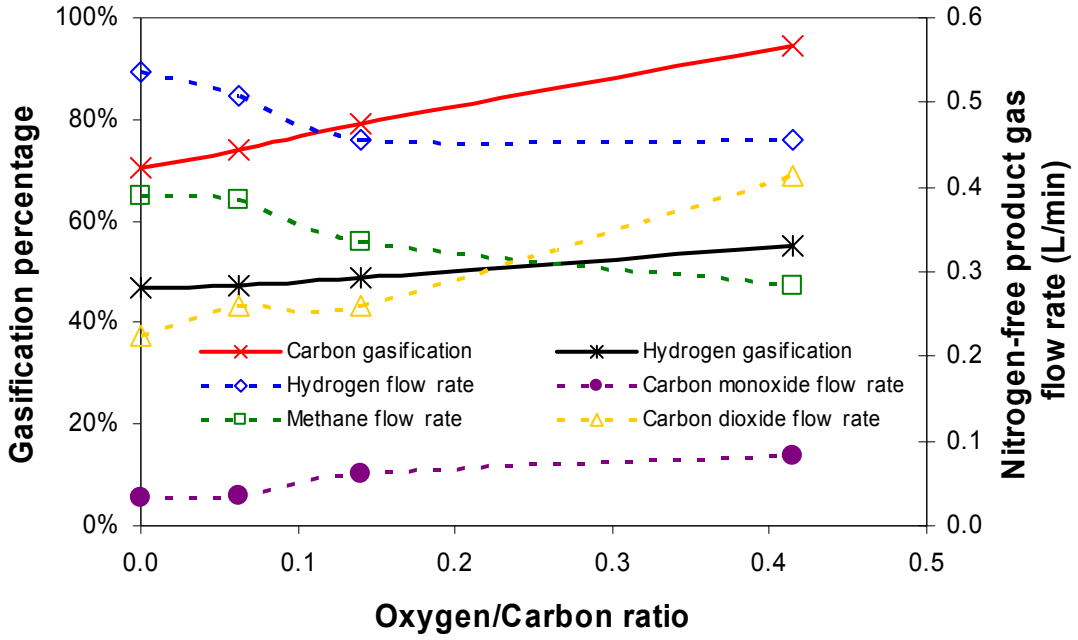

Figure 5-3. Nitrogen-free product gas flow rate and gasification percentage as a function of oxygen-to-carbon molar feed ratio. Experimental conditions, T = 764±2°C, P = 24.1±0.1 MPa, space time = 151±10 sec.

The hydrogen gasification percentage also increases linearly with the increasing O_2/C ratio, starting at 47% when no oxygen was present and increasing to 55% for the highest oxygen-to-carbon ratio, an 18% increase. The hydrogen gasification percentage increases with the increasing O_2/C ratio, even though the hydrogen gas flow rate was decreasing, because the gasification percentage is based on all the oxygen being consumed via partial oxidation, which stoichiometrically makes less hydrogen than

reformation. The decrease in the hydrogen gas flow rate from 0.54 to 0.46 L/min, a 15% decrease, could be due to partial oxidation, or from some of the oxygen consuming the hydrogen gas and producing water. The methane flow rate decreases from 0.39 to 0.28 L/min, a 27% reduction, was most likely a result of the oxidation reactions consuming fuel that would have otherwise undergone pyrolysis and become methane and coke, or from oxidation of the pyrolysis products. There was no ethane present in the gaseous effluent at this space time. The oxidation reactions are responsible for the increase in the oxygenated carbon compounds, carbon dioxide and carbon monoxide. The carbon monoxide flow rate increased 155% from no oxygen present to an oxygen-to- carbon ratio of 0.4, while the carbon dioxide flow rate increased by 84% over the same interval.

For a space time of 75±4 seconds, Figure 5-4 illustrates the effects of adding air to the system. The hydrogen and carbon gasification percentages do not increase linearly as they did in the 151±10 second space time experiments, but instead stay relatively steady for the first three oxygen-to-carbon ratios, then increase. The carbon gasification percentage starts at 71% when no oxygen was present, drops to 68%, then increases to 71% before finally ending up at 87% for the highest oxygen-to-carbon ratio. Hydrogen gasification has a similar trend, beginning at 44%, then mildly decreasing to 42% for the next two O_2/C ratios before increasing to 49% for the highest oxygen-to-carbon ratio. This lag in gasification response to the increasing oxygen level could be from the oxygen oxidizing species already present in the gas phase, such as methane and hydrogen, and not the jet fuel and solid carbon, or because reformation of the solid carbon was less active or appreciable at this shorter space time.

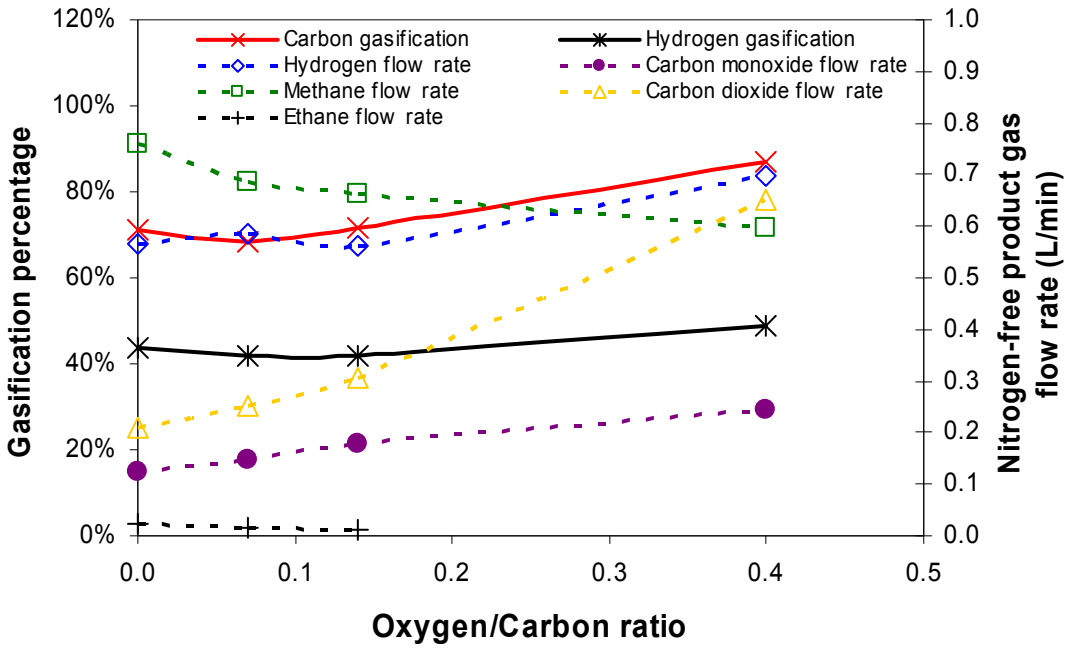

Figure 5-4. Nitrogen-free product gas flow rate and gaseous conversion as a function of oxygen-to-carbon molar feed ratio. Experimental conditions, T = 770±3°C, P = 24.1±0.1 MPa, space time = 75±4 sec.

The gas flow rate has also changed compared with the previous experiment. The H_2 flow increases with increasing oxygen, 23% from when no oxygen was present to a 0.4 O_2/C ratio, while for the 151±10 second space time experiments it decreased. This holds open the possibility that with even higher oxygen-to-carbon ratios there could be further increases in hydrogen, carbon dioxide and carbon monoxide flow rates and carbon conversion. The methane and ethane flow rates decreased with the increasing oxygen-to-carbon ratio, which could be due to the oxidation reaction consuming fuel that would have undergone pyrolysis and become gaseous hydrocarbons and coke, or oxidation creating smaller hydrocarbons that are more likely to be reformed than undergo pyrolysis. The creation and subsequent reformation of these smaller hydrocarbons could also explain the increasing hydrogen flow rate. The carbon monoxide flow rate increased by

100%, while the carbon dioxide flow rate increased by 210%, which was likely due to the oxidation reactions.

Experiments varying the oxygen-to-carbon ratio were also performed at a space time of 37±2 seconds, the results of which are illustrated in Figure 5-5. The hydrogen and carbon gasification percentages increase at the oxygen-to-carbon ratio of 0.07, then decrease. Hydrogen gasification increases from 30% to 39%, a 29% increase, and then drops to 34%, a 13% decrease. Carbon gasification was even more dramatic, going from 50% to 68% at the O_2/C ratio of 0.07, a 37% increase, then dropping 9% to a gasification percentage of 62%. This kind of sudden increase then decrease in conversion was unseen in the previous two space times that were studied. It was due to an increase in the methane and ethane flow rates, since the other flow rates are not changing as dramatically. Methane increased by 22% and ethane increased by 64% over the interval in question. Gaseous hydrocarbons are thought to be the by-products of pyrolysis, but elucidation of this specific condition as to why it would be more conducive to pyrolysis than the two surrounding data points would require more detailed analysis.

Excluding the increase at the 0.07 O_2/C ratio point, there are some similar trends compared to the previous two space times examined. Hydrogen gasification increases from 30% to 43% over the entire interval, a 42% increase. The carbon conversion also increases with the increasing O_2/C ratio, from 50 to 86%, a 72% increase, which is consistent with the previous experiments and is indicative of an increase in the oxidation reaction. The hydrogen flow rate increases from 0.70 to 0.86 L/min, a 22% increase, which is comparable to the percentage increase for the 75 second space time experiments over the same interval. The increasing carbon monoxide and carbon dioxide flow rates,

222% and 333%, respectively, again illustrate the increasing oxidation reaction as the O_2/C ratio increases. The methane flow rate stays nearly unchanged at about 1.1 L/min, while for the longer space time experiments the methane flow rate decreased due to the oxygenation and further reformation reactions competing with the pyrolysis reaction. This space time of 37 seconds could be too short to allow much reformation to occur, which would explain the steady flow rate of methane and ethane, while for the longer space times these gasses decreased with increasing oxygen-to-carbon ratio.

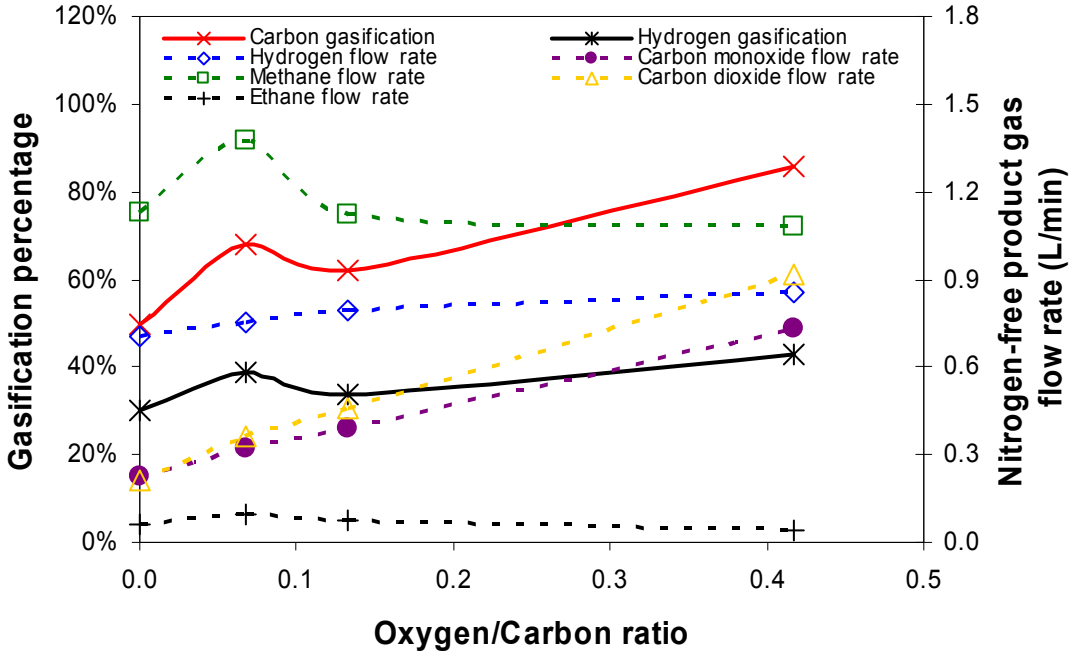

Figure 5-5. Nitrogen-free product gas flow rate and gaseous conversion as a function of oxygen- to-carbon molar feed ratio. Experimental conditions, T = 770±4°C, P = 24.16±0.03 MPa, space time = 37±2 sec.

In general, the space time of 151±10 seconds had the highest hydrogen and carbon conversion, and the highest hydrogen gas flow rate per gram of fuel fed. The

addition of air increased the carbon conversion, and the carbon monoxide and carbon dioxide concentration for all space times. Table 5-2 shows that the shorter space time experiments made less hydrogen per gram of fuel, but when the amount of carbon monoxide produced at the higher oxygen-to-carbon ratios is considered, the shorter space time experiments become more competitive.

Table 5-2. Hydrogen and carbon monoxide produced per gram of fuel for each experiment.

Experimental ID	Air flow (slpm)	Space time (sec)	Liter of H_2 gas produced per gram of fuel fed	Liter of H_2 and CO gas produced per gram of fuel fed
3	0.00	159	1.00	1.06
4	0.25	153	0.95	1.02
7	0.50	156	0.95	1.08
6	1.50	136	0.95	1.12
11	0.00	79	0.61	0.74
10	0.50	77	0.61	0.77
9	1.00	74	0.59	0.78
8	3.01	70	0.70	0.94
1	0.00	39	0.36	0.47
12	1.00	39	0.39	0.55
2	1.99	36	0.40	0.59
5	5.99	34	0.45	0.83

When considering carbon monoxide production, it must be remembered that the water gas shift reaction, Equation (2), can convert carbon monoxide to hydrogen, so carbon monoxide, while not as desirable as hydrogen, is almost as advantageous. A separate water gas shift reactor would have to be used, but the technology behind the WGS reaction is well understood.[43] Comparing experiments 5 and 6, the hydrogen gas

production was 53% less from experiment 6 to 5, but only 26% less when considering carbon monoxide production as well. The space time of experiments 6 was four times greater than that for experiment 5, while the oxygen-to-carbon ratio was the same.

6. SUMMARY AND CONCLUSIONS

6.1. SUMMARY

Targeted experiments were performed to determine the effects that reaction time and oxygen co-feed have on the novel non-catalytic reformation of jet fuel in supercritical water. The reformation of jet fuel was studied in a 0.4-L Haynes Alloy 230 tubular flow reactor. The goal was to produce hydrogen via reformation and partial oxidation, with partial oxidation also providing *in-situ* heat generation, non-catalytically due to the high sulfur content of aviation fuel. Three predetermined space times were tested at 39, 79 and 159 seconds under similar supercritical water process conditions of about 770°C, 24.1 MPa, and with a fifteen-to-one water-to-fuel feed ratio by weight. Various oxygen flow rates were also employed to examine the effects of oxidation on the system. The final, production-ready product would have hydrogen being ultra-purified and fed to a fuel cell to produce electric power; the system is envisioned as a mobile electricity generation unit to be used in the military as an alternative to generators, hence the use of military logistic jet fuel. The advantages over generators would be quieter operation with a smaller heat signature, both important factors in military applications.

6.2. CONCLUSIONS

A number of conclusions may be drawn from this experimental study. Without oxygen, as the space time increases from 39 to 79 seconds, hydrogen gasification increases from 30% to 44%, a 45% increase. Carbon gasification increases from 50% to 71%, a 43% increase over the same period. When the space time was doubled again,

from 79 to 159 seconds, the change was not as dramatic. Carbon gasification decreases to 70%, while hydrogen increases by 7% to 47%. It appears that some sort of limit has been reached where increasing space time no longer has such a pronounced effect upon gasification when no oxygen was present. All the carbon that was not gasified remains as solid in the reactor, based on liquid analysis and mass balances. While the carbon that becomes solid stays in the reactor, the gaseous hydrocarbons are reformed at the longer space times, indicated by the drop in methane and ethane concentration as space time increases, meaning these gaseous hydrocarbons are reformed preferentially over the solid hydrocarbon residues. The water gas shift reaction may also be more active at the longer space times based on the drop in carbon monoxide and increase in carbon dioxide and hydrogen gas concentration.

When air was added to the system, in general carbon and hydrogen gasification increased with increasing air flow. The increase in carbon gasification is at least partially attributable to the increased oxidation reaction, which would also explain the increase in carbon monoxide and dioxide flow rates as the oxygen-to-carbon ratio increased. These trends are present in all three of the space times studied. The increase in carbon gasification is important because if it is less than 100%, the remainder is left in the reactor as solid, which over time may prove problematic, such as clogging outlet lines or increasing wear on certain components. At a space time of 136 seconds, and an oxygen-to-carbon ratio of 0.4, carbon gasification was 94%, an increase of 38% compared to the nominally same experiment without oxygen. The highest carbon and hydrogen gasification percentage, as well as the highest concentration of hydrogen gas, occurred during the longest space time experiments and decreased as space time decreased when

comparing the experiments with equivalent oxygen-to-carbon ratios. Except for the 37-seconds space time experiments, the methane and ethane flow rates decreased for increasing oxygen, which could be due to the oxidation reaction consuming fuel that would have undergone pyrolysis and become gaseous hydrocarbons and coke, or oxidation creates smaller hydrocarbons that are more likely to be reformed than undergo pyrolysis.

When considering the amount of hydrogen produced per gram of fuel, the highest amount was produced at a space time of 159 seconds without any oxygen. The addition of oxygen decreases the amount of hydrogen produced per gram of fuel for the 150 second space time experiments, but increased it for the other two, shorter, space times. The addition of oxygen also increased the amount of carbon monoxide produced, which could easily be converted into hydrogen via the water gas shift reaction. If the combined production of hydrogen and carbon monoxide per gram of fuel is considered, the addition of oxygen is even more beneficial.

Comparing the effects of space time and oxygen-to-carbon ratio, space time effects the production of hydrogen more than the addition of air. A longer space time will produce more hydrogen gas. The addition of air effects the carbon gasification more than space time. As space time increases, carbon gasification does not always increase, but the addition of increasing amounts of oxygen does increase the carbon gasification. If the goal is to produce more hydrogen, increase the space time; if the goal is too increase carbon gasification and decrease coking, increase the oxygen-to-carbon ratio.

6.3. RECOMMENDATIONS FOR FUTURE WORK

Because of the numerous variables inherent to this process, it was necessary in this study to vary only a few conditions and have the rest remain constant. The oxygen-to-carbon ratio and the space time were changed, but the pressure, temperature, fuel-to-water ratio, and fuel type were kept constant. In future work, the effects of these parameters warrant further study. The air flow rate in future experiments could also be increased, to establish when 100% of the carbon is gasified and what effects even higher oxygen levels have on the products. A more detailed analysis of the energy requirements could be undertaken. Different fuel types could be used, or some of the product gasses like methane or carbon monoxide could be studied under supercritical water conditions. Most importantly, the mechanisms and rates for all the participating reactions need to be elucidated and quantified.

APPENDIX A

GAS CHROMATOGRAPH RUN CONDITIONS AND CALIBRATION

An HP 5890 Series A gas chromatograph (GC) equipped with a 15' by 1/8" stainless steel 60/80 Carboxen 1000 packed column is connected to a thermal conductivity detector (TCD). Two different methods are used when a sample is injected with a syringe, Air02 and Air03, while Loop05 is used with the Valco 16-port sampling loop. Each method, with its corresponding GC conditions, is described in Table A.1 below. The injection port on the GC is at a constant temperature of 120°C, and the TCD temperature is 220°C for each method.

Table A.1 GC conditions and times for gas sample methods.

GC Conditions	**Methods**		
	Air02.M	**Air03.M**	**Loop05.M**
Initial oven temperature (°C)	40.0	40.0	40.0
Initial time (min)	8.0	8.0	10.0
Level 1 Rate (°C/min)	20.0	20.0	8.0
Level 1 temperature (°C)	140.0	140.0	140.0
Level 1 time (min)	7.0	7.0	7.5
Level 2 Rate (°C/min)	N.A.	20.0	10.0
Level 2 temperature (°C)	N.A.	200.0	200.0
Level 2 time (min)	N.A.	10.5	13.0

Air02.M starts with an initial oven temperature of 40°C for 8 minutes, then ramps up to a temperature of 140°C at a rate of 20°C/min. The oven stays at this temperature for seven minutes, at which time the analysis is over and the oven cools back down to 40°C. In this time, hydrogen, nitrogen, carbon monoxide, methane and carbon dioxide are eluded from the column. As can be seen from Table A.1, Air03 is a continuation of

Air02. While Air02 stops at level 1, Air03 continues; after seven minutes at 140°C, the oven increases in temperature at 20°C/min until it reaches a temperature of 200°C, where it remains for 10.5 minutes. In this time, all of the previously mentioned species elude from the column, along with acetylene, ethylene and ethane. Loop05 detects the same species as Air03, but has different run conditions because of how the Valco 16-port sample loop is connected to the GC. The residence times at which all calibrated species elude are given in Table A.2.

Table A.2. Elution times for various species in the HP 5890 Series A gas chromatograph using method Air03.M.

Species	Elution time (min)	Standard Deviation
Hydrogen	2.3	0.1
Nitrogen	6.0	0.8
Carbon monoxide	7.0	0.4
Methane	12.1	0.2
Carbon dioxide	16.5	0.6
Acetylene	22.5	0.5
Ethylene	25.5	0.7
Ethane	28.8	0.9

The GC was calibrated for each of the species listed in Table A.2, and the results of that calibration are illustrated in the figures below. The number of moles in the injection was varied by changing the injection size, from 0.01 to 5 mL. The area is the area of the resulting peak, integrated by the HP Chemstation software.

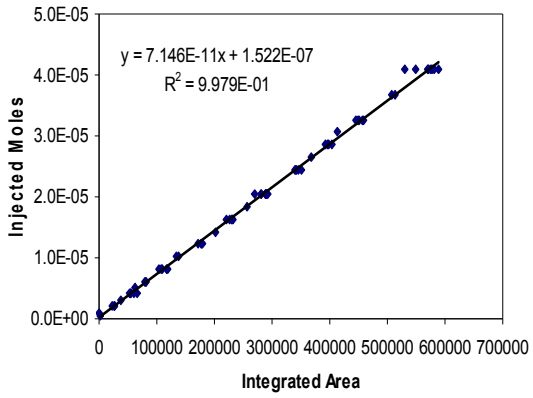

Figure A.1 Hydrogen gas calibration plot.

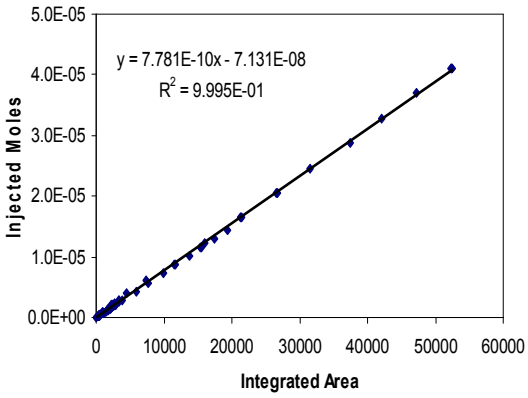

Figure A.3 Carbon monoxide gas calibration plot.

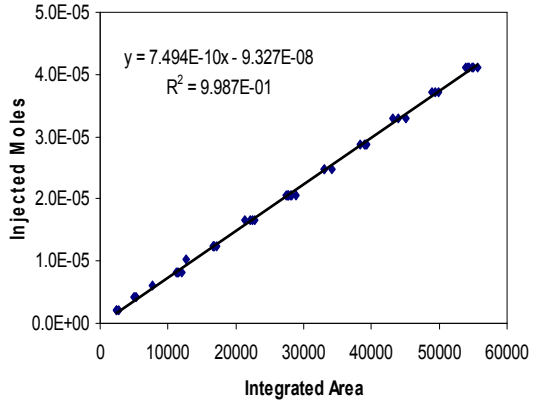

Figure A.2 Nitrogen gas calibration plot.

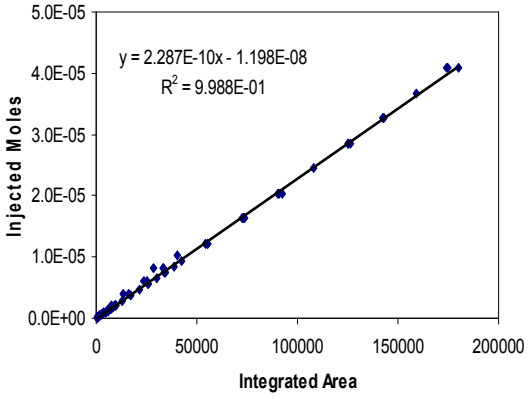

Figure A.4 Methane gas calibration plot.

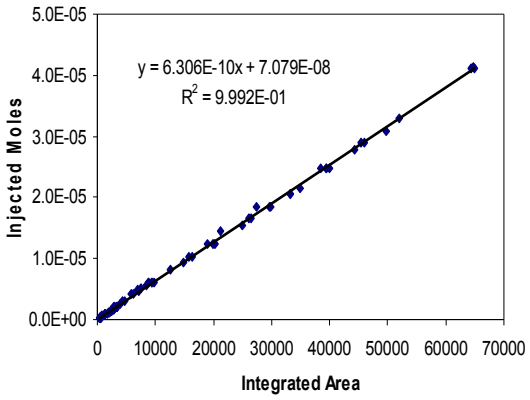

Figure A.5 Carbon dioxide gas calibration plot.

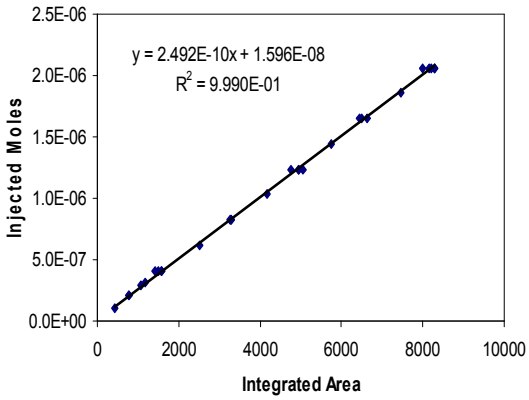

Figure A.7 Ethylene gas calibration plot.

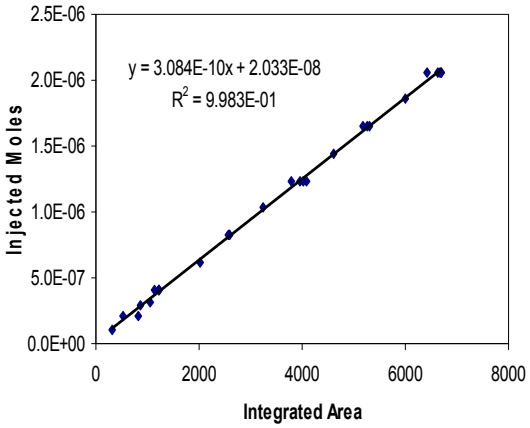

Figure A.6 Acetylene gas calibration plot.

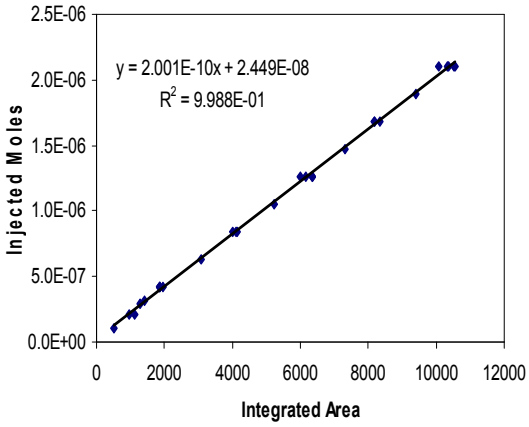

Figure A.8 Ethane gas calibration plot.

APPENDIX B

EXAMPLE OF AN HP CHEMSTATION REPORT

Below is an example of the reports that HP Chemstation generates upon completion of an analysis. This particular report is from November 30, 2006 and was the second gas sample syringe taken for Experiment #3. It was analyzed with method Air02, and from the areas reported here, and the calibrations given above, the mole percentage of each of the gasses was calculated. For the TCD, the gas species from left to right are: hydrogen at an elution time of 2.1 minutes, carbon monoxide at 7.0 minutes, methane at 12.0 minutes, and carbon dioxide at 16.4 minutes. The FID was not on, so no peaks were recorded for it.

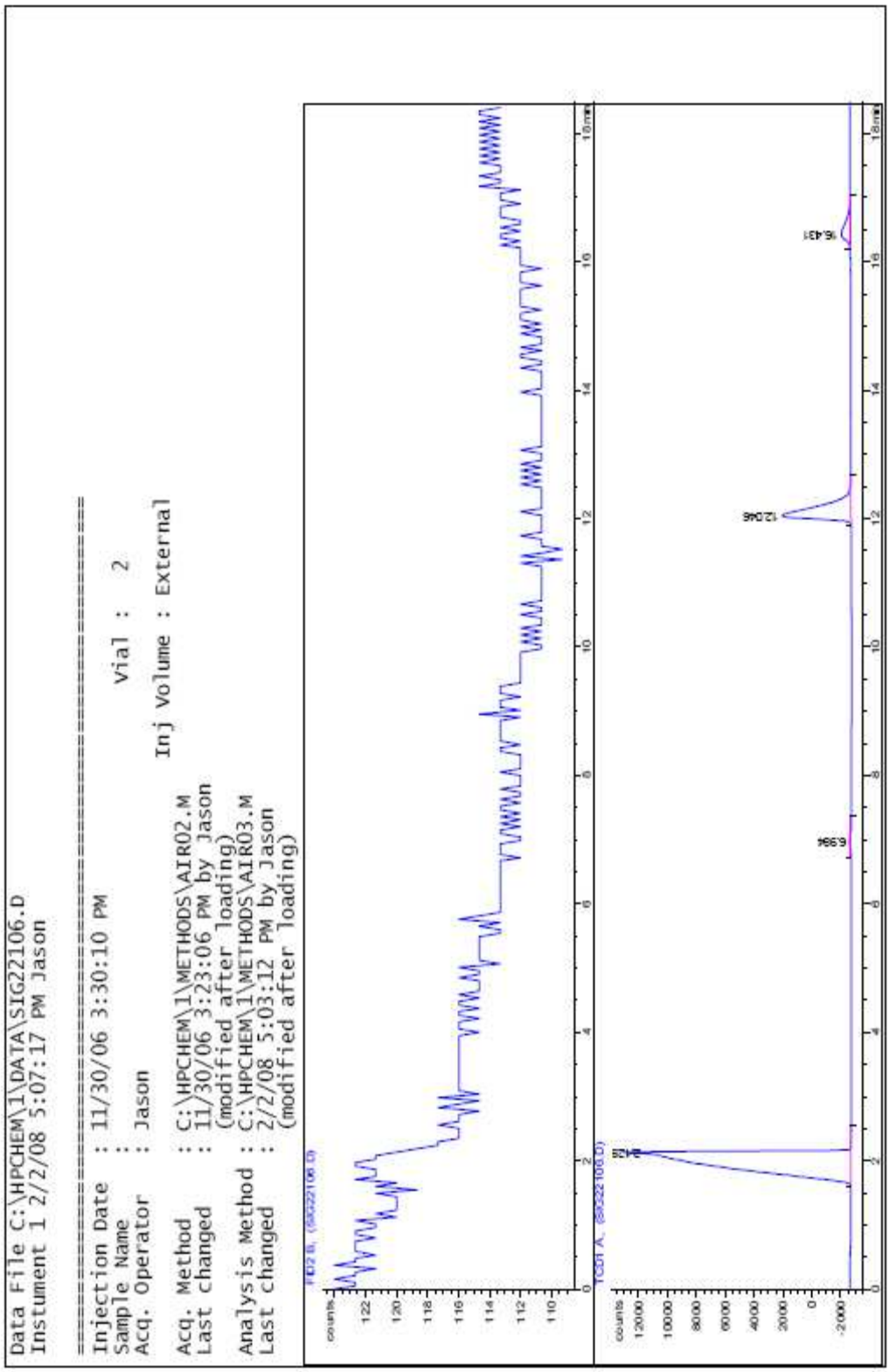
Data File C:\HPCHEM\1\DATA\SIG22106.D
Instument 1 2/2/08 5:07:17 PM Jason
Injection Date : 11/30/06 3:30:10 PM Vial : 2
Sample Name :
Acq. Operator : Jason Inj Volume : External
Acq. Method : C:\HPCHEM\1\METHODS\AIR02.M
Last changed : 11/30/06 3:23:06 PM by Jason
(modified after loading)
Analysis Method : C:\HPCHEM\1\METHODS\AIR03.M
Last changed : 2/2/08 5:03:12 PM by Jason
(modified after loading)
FID2 B, (SIG22106.D)
counts
FID1 A, (SIG22106.D)
6.984
12.046
16.431
min

Area Percent Report

Sorted By : Signal
Multiplier : 1.0000
Dilution : 1.0000

Signal 1: FID2 B,

Signal 2: TCD1 A,

Peak #	RetTime [min]	Type	Width [min]	Area counts*s	Height [counts]	Area %
1	2.128	BP	0.1915	2.50829e5	1.63002e4	77.27126
2	6.984	BP	0.1934	1565.02515	105.27240	0.48213
3	12.046	BB	0.1912	6.06824e4	4810.36133	18.69403
4	16.431	BB	0.2566	1.15320e4	621.05115	3.55259
Totals :				3.24608e5	2.18368e4	

Summed Peaks Report

Signal 1: FID2 B,
Signal 2: TCD1 A,

Final Summed Peaks Report

Signal 1: FID2 B,
Signal 2: TCD1 A,

*** End of Report ***

APPENDIX C

SPACE TIME CALCULATION USING THE PENG-ROBINSON EQUATION OF STATE WITH VAN DER WAALS MIXING RULES

The space time was based on the inlet reactant composition and calculated using the Peng-Robinson equation of state. The pressure used was the pressure recorded by the inlet pressure transducer, and the temperature was the average temperature measured by reactor thermocouples (RTC) four through eight. Because the inlet composition was a mixture of species, Van der Waals mixing rules were used to calculate the Peng-Robinson parameters *a* and *b*. The Peng-Robinson equation of state is

$$P = \frac{RT}{V-b} - \frac{a}{V(V+b)+b(V-b)}$$

P is the pressure, *T* is the temperature, *V* is the molar volume, and *a* and *b* are constants calculated using the Van der Waals mixing rules as follows

$$a = \sum\sum x_i x_j (1-k_{ij})(a_i a_j)^{0.5}$$

$$b = \sum y_i b_i$$

k_{ij} is an interaction parameter between the two species, and a_i and a_j designate *a* constants for the pure species, just as b_i is the *b* constant for that pure species, with x_i, x_j, and y_i representing the mole percent of that species *i* or *j*. a_i and b_i for each pure species is calculated from

$$a_i = 0.457235(R^2 T_{c_i}^2 / P_{c_i})[1 + F_i(1 - T_{R_i}^{0.5})]^2$$

$$b_i = 0.07796(RT_{c_i} / P_{c_i})$$

$$F_i = 0.37646 + 1.54226\omega - 0.26992\omega^2$$

Where T_{c_i} is the critical temperature, P_{c_i} is the critical pressure, T_{R_i} is the reduced temperature and w_i is the acentric factor for that particular species i. With a and b calculated for the mixture, the Peng-Robinson equation of state can be used to find V, the molar volume for the mixture, since the temperature and pressure of the reactor are known. The molar percents used to calculate a_i and b_i are the inlet molar percents, because the space time is calculated based on the inlet conditions. The molar inlet flow rate is known, and by multiplying the inlet molar flow rate by the molar volume, the volumetric flow rate is calculated. Dividing the volume of the reactor, 383 cm^3, by the volumetric flow rate in cm^3/min, gives the space time in minutes, from which it can be converted to seconds.

BIBLIOGRAPHY

1. Houghton, J. T.; Ding, Y.; Griggs, D.J.; Noguer, M.; van der Linden, P.J.; Dai, X.; Maskell, K.; Johnson, C.A., Eds. Contributions of Working Group I to the Third Assessment Report of the Intergovernmental Panel on Climate Change. *Climate change 2001: the Scientific Basis*; Cambridge Univ. Press, 2001.

2. Hydrogen Production, Energy Efficiency and Renewable Energy, U.S. Department of Energy. http://www1.eere.energy.gov/hydrogenandfuelcells/production/basics.html (accessed Dec 2007).

3. Holliday, R. L.; Jong, B. Y. M.; Kolis, J. W. Organic synthesis in subcritical water: Oxidation of alkyl aromatics. *J. Supercrit. Fluids* **1998**, *12*, 255-260.

4. Modell, M. Supercritical-Water Oxidation. In *Standard Handbook of Hazardous Waste Treatment and Disposal;* Freeman, H. M., Ed.; McGraw-Hill: New York, 1989; 8.153-8.168.

5. Los Alamos National Laboratory's Chemistry Division, Hydrogen fact sheet. http://periodic.lanl.gov/elements/1.html (accessed Dec 2007).

6. Hammond, C. R. The Elements. In *CRC Handbook of Chemistry and Physics*, 57th ed.; Weast, R.C., Eds.; CRC Press: Cleveland, OH, 1976; B-26.

7. The National Hydrogen Association, Frequently Asked Questions. http://www.hydrogenassociation.org/general/faqs.asp#howmuchproduced (accessed Dec 2007).

8. Hydrogen use in Internal Combustion Engines. In *Hydrogen Fuel Cell Engines and Related Technologies*, College of the Desert: Palm Desert, CA, Rev 0, 2001.

9. Mueller-Langer, F.; Tzimas, E.; Kaltschmitt, M.; Peteves, S. Techno-economic assessment of hydrogen production processes for the hydrogen economy for the short and medium term. *Int. J. of Hydrogen Energy* **2007**, *32,* 3797 – 3810.

10. Hydrogen Production-Steam Methane Reforming. In *Hydrogen Fact Sheet*, New York State Energy Research and Development Authority: Albany NY, 2004.

11. Beurden, V. P. *On the Catalytic Aspects of Steam-Methane Reforming, A Literature Survey*; Report ECN-I--04-033; Energy Research Center of the Netherlands: Petten, The Netherlands, 2004.

12. Ahmed, S. Water-Gas Shift Reaction over Cu-Based Mixed Oxide Catalysts. Proceedings of the 15th Saudi-Japan Joint Symposium, Dhahran, Saudi Arabia, Nov 27-28, 2005.

13. Picou, J.; Wenzel, J.; Lanterman, H. B.; Lee, S. Kinetics of Noncatalytic Water Gas Shift Reaction In a Supercritical Water Medium. Presented at the AIChE Spring National Meeting, New Orleans, LA, April 2008.

14. Ahmed, S.; Krumpelt, M.; Kumar, R.; Lee, S. H. D.; Carter, J.D.; Wilkenhoener, R.; Marshall, C.; Catalytic Partial Oxidation Reforming of Hydrocarbon Fuels. Presented at the 1998 Fuel Cell Seminar, Palm Springs, Ca, Nov 16-19, 1998.

15. Dogan, M.; Posarac, D.; Grace, J.; Adris, A. M.; Lim C. J. Modeling of Autothermal Steam Methane Reforming in a Fluidized Bed Membrane Reactor. *International Journal of Chemical Reactor Engineering* **2003**, *1*, Article A2.

16. Haryanto, A.; Fernando, S.; Murali, N.; Adhikari, S. Current Status of Hydrogen Production Techniques by Steam Reforming of Ethanol: A Review. *Energy Fuels* **2005**, *19*, 2098-2106.

17. Krummenacher, J. J.; West, K. N.; Schmidt, L. D. Catalytic partial oxidation of higher hydrocarbons at millisecond contact times: decane, hexadecane, and diesel fuel. *Journal of Catalysis* **2003**, *215*, 332–343.

18. Colwell, R. F.; *Oil Refinery Processes; A Brief Overview;* Process Engineering Associates, LLC http://www.processengr.com/ppt_presentations/oil_refinery_processes.pdf (accessed Dec 2007).

19. *CCR Platforming Process For Motor Fuel Production*; UOP Report number 4523-2 0407R0Wd; UOP: Des Plaines, IL, 2007.

20. Lee, S.; *Alternative Fuels*; Taylor & Francis: Philadelphia, PA, 1996; 95-157.

21. Basic Research Needs for the Hydrogen Economy, Report from the Basic Energy Sciences Workshop on Hydrogen Production, Storage, and Use, US Department of Energy, Office of Science. Report prepared by Argonne National Laboratory, May 13–15, 2003 http://www.sc.doe.gov/bes/hydrogen.pdf (accessed Dec 2007).

22. Schlapbach, L.; Züttel, A. Hydrogen Storage – Material for Mobile Applications. *Nature* **2001**, *414*, 23-31.

23. Hydrogen Fuel Cells, U.S. Department of Energy Hydrogen Program. www.hydrogen.energy.gov (accessed Dec 2007).

24. Barendrecht, E. Electrochemistry of Fuel Cells. In *Fuel Cell Systems*; Blomen, L. J. M. J., Mugerwa, M. N., Eds.; Plenum Press: New York, 1993; 97- 109.

25. Lilac, W. D. Controlled Depolymerization of Polypropylene via Selective Partial Oxidation in a Supercritical Water Medium. Ph.D. Dissertation, University of Missouri-Columbia, Columbia, MO, Dec 1999.

26. *Encyclopedia Britannica*, 11th Ed.; Oxford University Press: Oxford, 1911; 5 vols.

27. Rubin, J. B.; Davenhall, L. B.; Taylor, C. M. V.; Sivils, L. D.; Pierce, T. CO_2-Based Supercritical Fluids as Replacements for Photoresist-Stripping Solvents; Internal Los Alamos National Laboratory paper, 1998.

28. Kraan, M.; Cid, M. V. F.; Woerlee, G. F.; Veugelers, W. J. T.; Witkamp, G. J. Dyeing of natural and synthetic textiles in supercritical carbon dioxide with disperse reactive dyes. *J of Supercritical Fluids* **2007**, *40*, 470-476.

29. Lack, E.; Seidlitz, H. Commercial scale decaffeination of coffee and tea using supercritical CO_2. In *Extraction of Natural Products Using Near Critical Solvents*; King, M. B., Bott, T. R., Eds.; Chapman and Hall: London, UK, 1993; 101-129.

30. Clark, K. L. Synthesis of Maleated Poly(vinylidene Fluoride) in Supercritical Carbon Dioxide Medium. Ph.D. Dissertation, University of Missouri-Columbia, Columbia, MO, May 2004.

31. Hong, G. T.; Spritzer, M. H. Supercritical Water Partial Oxidation. Presentation to the Department of Energy Hydrogen Program Annual Review, Berkeley, CA, May 19-22, 2003.

32. Boukis, N.; Diem, V.; Habicht, W.; Dinjus, E. Methanol Reforming in Supercritical Water. *Ind. Eng. Chem. Res.* **2003**, *42*, 728-735.

33. Guo, L. J.; Lu, Y. J.; Zhang, X. M.; Ji, C. M.; Guan, Y.; Pei, A. X. Hydrogen production by biomass gasification in supercritical water: A systematic experimental and analytical study. *Catalysis Today* **2007**, *129*, 275-286.

34. Bo, Y.; Chao-hai, W.; Cheng-sheng, H.; Cheng, X.; Jun-zhang, W. Hydrogen generation from polyvinyl alcohol-contaminated wastewater by a process of supercritical water gasification. *Journal of Environmental Sciences* **2007**, *19*, 1424-1429.

35. Lu, Y. J.; Guo, L. J.; Ji, C. M.; Zhang, X. M.; Hao, X. H.; Yan, Q. H. Hydrogen production by biomass gasification in supercritical water: A parametric study. *Int. J. of Hydrogen Energy* **2006**, *31*, 822-831.

36. Pinkwart, K.; Bayha, T.; Wolfgang, L.; Krausa, M. Gasification of diesel oil in supercritical water for fuel cells. *J. of Power Sources* **2004**, *136*, 211-214.

37. Modell, M. Processing Method for the Oxidation of Organics in Supercritical Water. U.S. Patent 4,338,199, 1982.

38. *Inconel alloy 625*; Publication Number SMC-063; Special Metals Corporation, Jan 2006; 1.

39. *Haynes 230 Alloy*; Report H-3000H; Haynes High-Temperature Alloys International, 2004; 1-3.

40. ASTM Standard D2887, 2006a, "Standard Test Method for Boiling Range Distribution of Petroleum Fractions by Gas Chromatography." ASTM International, West Conshokechen, PA.

41. Nohara, D.; Sakai, T. Kinetic Study of Model Reactions in the Gas Phase at the Early Stage of Coke Formation. *Ind. Eng. Chem. Res.* **1992**, *31*, 14-19

42. Flytzani-Stephanopoulos, M.; Qi, X.; Kronewitter, S. *Water-gas Shift with Integrated Hydrogen Separation Process*; Final Report to DOE, DE-FG2600-NT40819; Tufts University: Medford, MA, February 2004; 3-8.

43. Callaghan, C. A. Kinetics and Catalysis of the Water-Gas-Shift Reaction: A Microkinetic and Graph Theoretic Approach. Ph.D. Dissertation, Worcester Polytechnic Institute, Worcester, MA, March 2006.

VITA

Jason Wade Picou was born in St. Louis on November 4th, 1982. Jason graduated from Ste. Genevieve High School in May of 2001. In December of 2005 he graduated from the University of Missouri-Columbia with a B.S. in Chemical Engineering. Jason transferred to Missouri University of Science and Technology and graduated with his Master's Degree in Chemical Engineering in August 2008.